A Targeted Genome-scale Overexpression Platform for Proteobacteria

Authors

Amy B. Banta[1,2], Kevin S. Myers[2,3], Ryan D. Ward[1,2,4], Rodrigo A. Cuellar[5], Michael Place[2], Claire C. Freeh[1], Emily E. Bacon[1,5], and Jason M. Peters[1,2,6,7,8]✉

Affiliations

[1]Pharmaceutical Sciences Division, School of Pharmacy, University of Wisconsin-Madison, Madison, WI, USA. [2]DOE Great Lakes Bioenergy Research Center, University of Wisconsin-Madison, Madison, WI, USA. [3]Wisconsin Energy Institute, University of Wisconsin-Madison, Madison, WI, USA. [4]Laboratory of Genetics, University of Wisconsin-Madison, Madison, WI, USA. [5]Microbiology Doctoral Training Program, University of Wisconsin-Madison, Madison, WI, USA. [6]Department of Bacteriology, University of Wisconsin-Madison, Madison, WI, USA. [7]Department of Medical Microbiology and Immunology, University of Wisconsin-Madison, Madison, WI, USA. [8]Center for Genomic Science Innovation, University of Wisconsin-Madison, Madison, WI, USA. ✉e-mail: jason.peters@wisc.edu

Abstract

Targeted, genome-scale gene perturbation screens using Clustered Regularly Interspaced Short Palindromic Repeats interference (CRISPRi) and activation (CRISPRa) have revolutionized eukaryotic genetics, advancing medical, industrial, and basic research. Although CRISPRi knockdowns have been broadly applied in bacteria, options for genome-scale overexpression face key limitations. Here, we develop a facile approach for genome-scale gene overexpression in bacteria we call, "CRISPRtOE" (CRISPR transposition and OverExpression). We create a platform for comprehensive gene targeting using CRISPR-associated transposition (CAST) and show that transposition occurs at a higher frequency in non-transcribed DNA. We then demonstrate that CRISPRtOE can upregulate gene expression in Proteobacteria with medical and industrial relevance by integrating synthetic promoters of varying strength upstream of target genes. Finally, we employ CRISPRtOE screening at the genome-scale in Escherichia coli, recovering known antibiotic targets and genes with unexplored roles in antibiotic function. We envision that CRISPRtOE will be a valuable overexpression tool for antibiotic mode of action, industrial strain optimization, and gene function discovery in bacteria.

Introduction

Overexpression (OE) studies have been invaluable for gene phenotyping in medical[1–3], industrial[4], and basic contexts[3,5]. When used in functional genomics, OE enables functional interrogation of genes that are normally cryptic under screening conditions[3], mimics natural resistance mechanisms[3], and complements loss of function approaches by identifying genes with oppositely signed phenotypes when knocked down versus overexpressed[1,6]. Clustered Regularly Interspaced Short Palindromic Repeats activation (CRISPRa) has allowed routine, genome-scale overexpression screening in eukaryotes for drug synergy/antagonism[6] or sensitivity/resistance to toxic plant compounds that reduce bioproduct yields[7]. Such screens have been highly effective at identifying direct targets and pathways that mitigate or potentiate drug function. For example, a recent screen in mammalian cells for targets of the anti-cancer drug, rigosertib, leveraged genome-scale CRISPR interference (CRISPRi) knockdowns with CRISPRa to identify target pathways that showed oppositely signed phenotypes[1]. OE has also enhanced strain optimization for industrial purposes, such as a genome-wide CRISPRa screen in *Saccharomyces cerevisiae* for genes involved in resistance to the biofuel production stressor, furfural[7].

Existing genome-scale OE approaches in bacteria face key limitations. Classic approaches, such as random integration of promoter containing transposons to overexpress downstream genes[8], are untargeted and often require hyper-saturated transposon (Tn) libraries to resolve ambiguities related to the effects of Tn insertion versus overexpression. Open Reading Frame (ORF) libraries cloned into plasmids[9] are technically targeted approaches, but are tedious and expensive to construct, limiting their utility in non-model bacteria. Further, the use of plasmids presents additional complications, such as the constant requirement for antibiotic selection for maintenance (complicating antibiotic function screens), and copy number variation that increases experimental noise[10]. Contemporary approaches have sought to mitigate these issues and make genome-scale overexpression more accessible. For instance, trackable multiplex recombineering (TRMR) is a targeted approach that uses recombinase-aided DNA insertion (recombineering) to deliver barcoded promoters or ribosome binding site variants to systematically alter gene expression[11,12]; however, this method is restricted to bacteria with efficient recombineering systems. An innovative new OE technique, “Dub-seq,” uses random genomic fragments cloned into multi-copy plasmids that can be quantified by barcode sequencing[13,14], reducing upfront barriers to library design, but complicating downstream analysis and sharing some downsides with other plasmid-based approaches. Moreover, the length of cloned genomic fragments dictates Dub-seq library screening results;

67 smaller fragments may miss genes that only have phenotypes when co-expressed in operons
68 (e.g., protein complex subunits) while longer fragments make it more difficult to pinpoint
69 individual genes responsible for the selected phenotype.
70 CRISPRa in eukaryotes uses a catalytically inactive Cas9 protein (dCas9) and single
71 guide RNAs (sgRNAs) to deliver activator proteins to promoters; these activators open
72 chromatin at the promoter, enhancing transcription activation[15]. In contrast, CRISPRa-based OE
73 in bacteria requires direct interactions between activator proteins and RNA polymerase (RNAP)
74 that dictate stringent activator-RNAP spacing and orientation on DNA[16–19]. Recent
75 improvements to bacterial CRISPRa using dCas9 variants with reduced PAM stringency and
76 engineered activator proteins partially mitigated the spacing requirements and increased overall
77 activation[18,19]; however, even in these optimized systems, less than half of targeted promoters
78 could be upregulated[19]. Accordingly, to our knowledge, no genome-scale bacterial CRISPRa
79 screens have been reported.
80 Naturally occurring CRISPR-associated transposon (CAST) systems[20] have been
81 engineered to generate targeted insertions in bacterial genomes with high efficiency[21–23].
82 Although several CAST systems have been described[24–26], the Tn*6677* system from *Vibrio*
83 *cholerae* (VcCAST) is among the best characterized and most precise[27–30]. In VcCAST, a
84 nuclease-deficient Type I-F CRISPR system is paired with a Tn*7*-like transposase to achieve
85 guide RNA-directed transposition. Binding of a VcCAST-gRNA complex spacer to a matching
86 protospacer results in transposition of DNA flanked by Tn*6677* ends ~49 bp downstream of the
87 protospacer. Transposon DNA can be inserted in two orientations with respect to the Tn*6677*
88 ends (R-L or L-R) but is highly biased toward the R-L orientation[21,31]. VcCAST is highly precise,
89 with nearly all tested guides showing >99% on-target insertion. The utility of CASTs has been
90 demonstrated for high efficiency editing in Proteobacteria[21], systematically disrupting
91 transcription factor genes in *Pseudomonas aeruginosa*[23], and even targeting individual strains in
92 a complex microbiome[22], but existing systems remain sub-optimal for genome-scale functional
93 genomics. Moreover, the use of Tn*6677* to deliver regulatory elements—such as promoters—
94 has only recently been explored in a model bacterium[32].
95 Here we modify VcCAST for genome-scale functional genomics, creating a targeted
96 overexpression system for bacteria we call, "CRISPRtOE" (CRISPR transposition and
97 OverExpression). CRISPRtOE delivers a transposon with an outward facing promoter upstream
98 of genes to facilitate overexpression (Fig. 1a). We demonstrate the utility of CRISPRtOE in
99 medically and industrially-relevant Proteobacterial species and at the genome-scale in
100 *Escherichia coli* to characterize antibiotic action and resistance.

101

102 # Results

103 ## A VcCAST Platform for Genome-scale Functional Genomics

104 We first generated "CRISPRt," a VcCAST system designed for genome-scale functional
105 genomics. Like previous VcCAST systems[21,22], CRISPRt enables precise insertion of
106 transposons into genomic targets using programmable gRNAs (Fig. 1b). Superimposed on this
107 are additional properties necessary for facile use of CRISPRt screening at the genome-scale: 1)
108 Tn insertion is selectable, resulting in all transconjugants containing an integrated Tn; 2) *cas*
109 helper and Tn plasmids are non-replicative in recipient bacteria, obviating the need for plasmid
110 curing[23] prior to phenotyping; 3) *cas* and Tn components are on separate plasmids, preventing
111 insertion of *cas* genes into the genome in rare events when VcCAST co-integrates the plasmid
112 backbone alongside the Tn (occurring at ~0.01-0.001% frequency) and reducing Tn plasmid
113 size which facilitates conjugation and cargo modification by standard cloning procedures (Fig.
114 1a, 1b, 1c, and Supplementary Fig. S1a, S1b, and S1c). CRISPRt can be transferred from
115 donor *Escherichia coli* K-12 cells to recipient Proteobacteria (and possibly other phyla) *via*
116 conjugation, and transconjugants containing Tn insertions are recovered at efficiencies
117 consistent with genome-scale library creation.

118 To test the precision of CRISPRt, we targeted both endogenous (*lacZ*) and heterologous
119 (*gfp*) reporter genes for disruption in *E. coli* K-12 (Supplementary Fig. S1d). Consistent with
120 previous data on VcCAST systems, we found that the vast majority of Tn insertions were on-
121 target. We first assessed targeting of *gfp* and *lacZ* using phenotypic assays (fluorescence
122 measurements for *gfp* and blue-white screening for *lacZ*), finding that 97.6% and 100% of
123 transconjugants showed the expected disruption phenotype, respectively (Supplementary Fig.
124 S2a and S2b). Next, we measured targeting on the genome scale by sequencing genomic DNA
125 at the Tn*6677* transposon junction (Tn-seq) using Illumina-based Next Generation Sequencing
126 (NGS). Tn-seq showed >99.5% on target efficacy for both *gfp* and *lacZ* guide RNAs (Fig. 1d). As
127 expected, Tn insertions largely occurred in a tight window centered at ~49 bp downstream of the
128 protospacer that favored an R-L orientation (89.2% and 74.1% R-L for *gfp* and *lacZ*,
129 respectively, (Fig. 1d and 1e)). Moreover, CRISPRt transconjugants were recovered at an
130 efficiency compatible with genome-scale screening (~10^{-2} to 10^{-3} in *E. coli*, (Supplementary Fig.
131 S2c)). We conclude that CRISPRt has excellent properties for functional genomics while
132 retaining the on-target efficacy of VcCAST.

133

CRISPRt Efficacy is Higher on Non-transcribed DNA

Although Protospacer Adjacent Motif (PAM) requirements for VcCAST have been well characterized (a "CN" PAM is sufficient[25]), other genomic features that impact guide efficacy are poorly understood. To address this issue, we created a pooled CRISPRt library targeting both strands of an *mScarlet-I* reporter gene that was integrated into the genome of *E. coli* K-12 (46 gRNAs total (Fig. 2a)). Surprisingly, we found that guide efficacy depended on which strand was targeted. To measure relative guide efficacy, we compared the abundance of gRNA spacers in our library before and after transposition into *mScarlet-I* (i.e., in mating donor strains versus recipient transconjugants (Fig. 2b)). Consistent with previous data from smaller sets of spacers[33], we found considerable variability, with ~27-fold difference in efficacy between the most and least active guides. We noticed a clear, but not absolute bias toward higher efficacy in template strand targeting guides (i.e., gRNAs that bind the transcribed strand) versus those that targeted the non-template strand. Other variables, such as PAM identity or distance from the gene start did not show an obvious trend (Supplementary Fig. S3a and S3b).

The bias in strand specificity suggested that either replication or transcription could be impacting CRISPRt efficacy. To test for a replication effect, we flipped the orientation of *mScarlet-I* relative to the origin or replication (Supplementary Fig. S3c). However, we continued to observe strand specificity in the flipped target, seemingly ruling out a role for replication direction in CRISPRt efficacy (Supplementary Fig. S3d and S4a). To test for a transcription effect, we targeted a promoterless version of *mScarlet-I* with our CRISPRt library (Supplementary Fig. S3c). In contrast to the transcribed target, the promoterless *mScarlet-I* gene showed reduced variation in guide efficacy, consistent with transcription affecting CRISPRt function (Supplementary Fig. S3c and S4a). Because our pooled approach did not allow for an absolute measure of CRISPRt activity, we cloned the three most active guides from our *mScarlet-I* library (T03, T09, and T21) and individually tested their activities (Fig. 2c and Supplementary Fig. S4b). We found that transcription reduced recovery of CRISPRt transconjugants (transposition efficiency) by 6.9 to 19.6-fold, depending on the guide tested. Although Tn disruption of transcribed genes is effective, we conclude that CRISPRt efficacy increases on non-transcribed targets.

Targeted and Tunable Overexpression in Proteobacteria

We considered that CRISPRt could be modified into an overexpression system by inserting outward-facing promoters into the Tn*6677* transposon that would cause increased transcription

167 of downstream genes (CRISPRtOE (Fig. 3a)). We inserted synthetic, constitutive promoters of
168 varying strength that had been shown to function in various Proteobacteria[34,35] into Tn*6677* with
169 the goal of creating an OE gradient (Supplementary Fig. S5a and S5b). To quantify the OE
170 activity of CRISPRtOE, we generated a "test" strain with a promoterless *mScarlet-I* reporter
171 gene integrated into the *E. coli* K-12 genome. This cassette contained a well-characterized
172 protospacer upstream of *mScarlet-I* to act as a "landing pad" (LP) for CRISPRtOE transposons
173 (Fig. 3a and Supplementary Fig. S5c). The test strain showed negligible mScarlet-I expression
174 in the absence of an upstream CRISPRtOE insertion (Fig. 3b).
175 CRISPRtOE achieved a gradient of mScarlet-I overexpression across our series of
176 tested promoters (Fig. 3b). CRISPRtOE containing the strong P_H promoter showed a ~177-fold
177 increase in mScarlet-I expression, while weaker promoters showed intermediate increases.
178 CRISPRtOE lacking a promoter (no P) failed to stimulate transcription above background,
179 although we note that insertions in the reverse orientation (L-R) were excluded from this
180 analysis due to cryptic promoter activity (Supplementary Fig. S6a and Table S8). We also
181 observed small variations in overexpression depending on the precise location of insertion,
182 possibly due to changes in mRNA folding (Supplementary Table S8).
183 We next sought to demonstrate CRISPRtOE activity in Proteobacteria with medical and
184 industrial relevance. The Alphaproteobacterium, *Zymomonas mobilis*, is a promising biofuel
185 producer and emerging model for bacteria with naturally reduced genomes[36]. To assay
186 CRISPRtOE function in *Z. mobilis*, we again generated an *mScarlet-I* test strain and measured
187 expression following insertion of CRISPRtOE transposons (Supplementary Fig. S6b and Table
188 S8). We found that CRISPRtOE could produce a gradient of overexpression in *Z. mobilis* up to
189 ~50-fold. Differences in the fold effects of CRISPRtOE across species likely reflect variation in
190 promoter activity among our constitutive promoter set.
191 We then extended this approach to a panel of eight total species including the Gram-
192 negative ESKAPE pathogens[37] *Klebsiella pneumoniae*, *Acinetobacter baumannii*, *P. aeruginosa*,
193 and *Enterobacter cloacae*, as well as the industrially and environmentally relevant strains
194 *Pseudomonas putida*[38] and *Shewanella oneidensis*[39], focusing our strongest promoter (P_H) to
195 reduce experimental complexity (Fig. 3c and Supplementary Table S8). We found that
196 CRISPRtOE could upregulate *mScarlet-I* expression in all tested species with an
197 overexpression range of 232-fold (*E. cloacae*) to 23-fold (*P. aeruginosa*), likely due to variation
198 in promoter activity across species. The CRISPRtOE insertion position in most species was
199 centered at 33 bp upstream of *mScarlet-I*, although *A. baumannii* showed a wider range of
200 positions for unknown reasons (Supplementary Fig. S6c). We note that the modular design of

201 CRISPRtOE enables facile swapping of promoter sequences with organism-specific or inducible
202 promoters to customize expression levels depending on the application. We conclude that
203 CRISPRtOE is an effective overexpression strategy for Proteobacteria.
204

205 Pooled CRISPRtOE Recapitulates Known Antibiotic Targets

206 There is an urgent need to develop new therapeutics to stem the rising tide of antibiotic
207 resistance[40]. One major bottleneck in the process of translating new antimicrobials to the clinic
208 is determining the mode of action (MOA), including identifying the direct target. We previously
209 showed that CRISPRi could be used to determine the direct targets of uncharacterized
210 antibiotics by observing synergy between knockdown strains and sub-lethal concentrations of
211 antibiotic[41,42]. However, CRISPRtOE could provide an even more straightforward avenue to
212 antibiotic target discovery because strains with overexpressed target proteins would outgrow
213 competitor strains in a pooled context. For instance, it has been shown that OE of *folA*,
214 encoding the trimethoprim (TMP) target, Dihydrofolate reductase (DHFR), can substantially
215 increase resistance to TMP[43]. Likewise, *murA*, encoding the fosfomycin (FOS) target, UDP-NAG
216 enolpyruvyl transferase (MurA), can provide FOS resistance when overexpressed[44].
217 To validate CRISPRtOE as a tool for functional interrogation of endogenous genes and
218 antibiotic target discovery, we overexpressed and phenotyped the *folA* and *murA* genes in *E.*
219 *coli* K-12. As a hedge against variation in integration efficiency and overexpression efficacy, we
220 tiled the region upstream of *folA* and *murA* with 12 unique spacers per gene and created a
221 negative control library that inserted into the *lacZ* coding region (Fig. 4a). To test for
222 overexpression phenotypes, we mixed our *folA* or *murA* library 50:50 with the *lacZ* control library
223 and grew cells in the presence/absence of TMP or FOS, respectively. Strikingly, we found that
224 all CRISPRtOE gRNA spacers targeting *folA* or *murA* were effective in increasing competitive
225 fitness in the context of TMP or FOS, respectively (Fig. 4b and Supplementary Fig. S7a). This
226 competitive advantage led to a 22-fold increase in the abundance of *folA* OE strains and a 52-
227 fold increase in *murA* OE strains, relative to *lacZ* controls. To further characterize the impact of
228 CRISPRtOE on TMP and FOS resistance, we performed Minimal Inhibitory Concentration (MIC)
229 strip assays on individual insertion isolates (Supplementary Fig. S7b, S7c, and S7d).
230 CRISPRtOE strains showed dramatically increased resistance, in some cases with an MIC
231 change that approached the maximum value of the scale. Because FOS showed a high
232 frequency of spontaneous resistant suppressors in MIC strip assays, we focused on TMP in
233 subsequent broth microdilution MIC measurements including the wild-type parent strain, a *lacZ*
234 negative control, and *folA* CRISPRtOE isolates with insertions at various positions upstream of

235 *folA* (due to different spacer usage (Fig. 4c)). We observed substantial shifts in MIC (~15 to 30-
236 fold) between the parent strains and *folA* CRISPRtOE isolates, demonstrating that CRISPRtOE
237 phenotypes were robust to insertion distance upstream of the target gene. We conclude that
238 CRISPRtOE reliably upregulates endogenous target genes and can recapitulate antibiotic
239 targets.
240

241 Genome-scale CRISPRtOE Reveals Antibiotic Targets and Resistance 242 Pathways

243 Buoyed by our success with *folA* and *murA*, we expanded the scope of our pooled CRISPRtOE
244 screening to the genome-scale. We targeted all protein coding genes in the *E. coli* K-12 genome
245 with ~10 gRNAs designed to integrate CRISPRtOE transposons within a small window
246 upstream of genes without disrupting downstream coding sequences (45,767 guides total, (Fig.
247 5)). Critically, we generated two pooled libraries, with and without promoter H, that allowed us to
248 distinguish between effects caused by promoter activity (intended overexpression) versus
249 upstream gene disruption (unintended loss of function). We found that CRISPRtOE effectively
250 targeted regions upstream of genes across the genome, without obvious hot spots or depleted
251 regions (Fig. 5a, see "CRISPRtOE No Promoter"). To characterize the insertion of CRISPRtOE
252 transposons relative to genes, we calculated the distance between transposon ends and gene
253 starts, finding a tight distribution of insertions largely within 100 bp of the 5′ ends of genes and
254 centered at ~20 bp upstream (Fig. 5b). This tight CRISPRtOE distribution showed a stark
255 contrast with the nearly flat distribution of Tn*5* insertions, which are known to occur pseudo-
256 randomly[45]. For instance, the distinction between CRISPRtOE targeted and Tn*5* pseudo-random
257 insertion was clearly visible at the *lac* locus (Fig. 5c).
258 To test the ability of CRISPRtOE to identify antibiotic-relevant gene phenotypes at the
259 genome-scale, we grew our libraries in the presence or absence of a sub-lethal concentration of
260 TMP and measured relative strain abundance. Biological replicates showed excellent
261 agreement at the gene level (R^2 values ranged from 0.95 to 0.97, Supplementary Fig. S8),
262 underscoring the high reproducibility of genome-scale CRISPRtOE. We found *folA*-associated
263 spacers as clear positive outliers (>1000-fold enrichment), demonstrating the exquisite
264 sensitivity and specificity of our CRISPRtOE screen in recapitulating antibiotic targets (Fig. 5a,
265 5d, and 5e). Substantial *folA* enrichment was only seen in the P_H-containing library not in the
266 promoterless library, indicating the CRISPRtOE promoter activity, rather than insertion per se,
267 was responsible for the phenotype (Fig. 5e). Promoter-dependent phenotypes were distinct

268 across the entire genome, as relative strain abundances of the P_H and no promoter libraries
269 after TMP treatment were not correlated (R^2 = 0.037, Supplementary Fig. S8). Importantly, we
270 were able to improve data quality by computationally eliminating aberrantly inserted
271 transposons based on distance between the intended target (defined by the spacer sequence)
272 and the insertion position/orientation (defined by Tn-seq). This mostly impacted our "no
273 promoter" data as cryptic transcription from transposons that inserted in the L-R orientation also
274 resulted in overexpression phenotypes (Supplementary Fig. S6). Our libraries contained many
275 more guides than was necessary to uncover phenotypes, as gene-level phenotypes were robust
276 when the number of spacers per gene was reduced from ~10 to just 3 (R^2 = 0.93,
277 Supplementary Fig. S9) and considering only guides that targeted the first gene of operons
278 returned many of the same top hits (Supplementary Fig. S10); these findings suggest that
279 CRISPRtOE library complexity can be reduced considerably with similar results. Thus, we
280 anticipate that future CRISPRtOE libraries will achieve genome-scale overexpression with far
281 fewer guides per gene.
282 Other significant outliers revealed potential TMP resistance or susceptibility mechanisms
283 (Fig. 5e and Supplementary Fig. S10). One of the most resistant outlier genes was *soxS*,
284 encoding an AraC-type transcription activator known to regulate genes involved in antibiotic
285 resistance[46] (Fig. 5e). Indeed, gene set enrichment analysis showed that several members of
286 the AraC and MarR families[47] were resistant outliers in our screen, including *marR*, *rob*, *soxR*,
287 and *marA* (FDR = 0.0055, afc test) (Fig. 5e and Supplementary Fig. S10), which notably
288 includes genes encoding the AcrA and AcrB components of the AcrAB-TolC multidrug efflux
289 pump[48]. Consistent with this, CRISPRtOE of the *acrA* gene also increased TMP resistance
290 (Supplementary Fig. S10). TMP treatment reduces cellular methionine levels due to the
291 involvement of tetrahydrofolate (the product of DHFR) in methionine biosynthesis[49].
292 CRISPRtOE of the *metR* gene, which encodes a positive regulator of methionine biosynthesis
293 genes[50], increased TMP resistance, possibly by increasing flux through the pathway. In contrast,
294 *metF* overexpression was highly deleterious in the presence of TMP (Supplementary Fig. S10),
295 likely due to depletion of 5,10-methylenetetrahydrofolate pools normally used by the ThyA-
296 DHFR pathway to generate tetrahydrofolate[51]. Neither *metR* nor *metF* were recovered in
297 previous TMP loss-of-function screens[52,53], demonstrating the utility of CRISPRtOE to identify
298 new players in antibiotic function. Interestingly, CRISPRtOE of *folM*, which is thought to encode
299 a protein with DHFR activity[54], was highly toxic to TMP-treated cells (Supplementary Fig. S10).
300 Although unintuitive, this result is consistent with other genome-scale phenotyping studies that
301 found that disruption of *folM* increases resistance to TMP[52,53]. Finally, genes involved in

302 biosynthesis of the Enteric Common Antigen (ECA), a key component of the enterobacterial
303 outer membrane, were functionally enriched among sensitive outliers (FDR = 5.58e-05, afc test)
304 (Supplementary Fig. S10). Previous work has shown that disruption of the ECA pathway also
305 increases TMP sensitivity, possibly by sequestering thymidine pools and leading to "hyper-
306 acting" version of thymine-less death[55]. Our work suggests that disregulation by overexpression,
307 in addition to disruption, can cause ECA-dependent toxicity in TMP-treated cells. Although ECA
308 genes often exist in complex operons that may be disrupted by insertion, phenotypes for some
309 ECA genes (e.g., *rffM*) were strongly dependent on the presence of P_H (Supplementary Fig.
310 S10). Future studies will be needed to define the precise mechanisms of TMP resistance and
311 sensitivity observed here. Taken together, genome-scale CRISPRtOE is a facile approach for
312 comprehensive genetic analysis of antibiotic function.
313

314 ## Discussion

315 Functional genomics approaches that are robustly scalable and readily applicable to diverse
316 bacteria are required to bridge the yawning gap between genome sequencing and gene function
317 assessment. Our work provides a targeted, systematic, and practical approach for genome-
318 scale gene overexpression in Proteobacteria and possibly beyond. By modifying VcCAST for
319 use in functional genomics (Fig. 1) and defining non-transcribed regions of DNA as high-
320 efficiency insertion sites (Fig. 2), we demonstrated targeted and tunable OE in Proteobacteria
321 with medical, industrial, and basic research relevance (Fig. 3). Our genome-scale OE screen for
322 targets and modulators of TMP efficacy highlighted the exquisite specificity of CRISPRtOE in
323 recovering genes and pathways that underpin antibiotic function (Fig. 4 and 5). Given the ease
324 of implementing CRISPRtOE in the organisms explored here, we anticipate that our approach
325 will be readily expandable to other microbes and screening conditions. While our manuscript
326 was under review, another manuscript was published that showed that VcCAST containing
327 promoters could be used to upregulate genes in *E. coli*[32]. Our work dramatically expands this
328 approach across multiple Proteobacteria and to the genome scale. We note that the replicative
329 CAST vector used in that study is suboptimal for use at the genome-scale due to a lack of Tn
330 selection, the need to cure the plasmid post-editing, and an inability to replicate in important
331 genera such as *Acinetobacter*.
332 CRISPRtOE is a valuable genetic tool for both basic and applied biology. The targeted
333 aspect of CRISPRtOE can be used to generate focused libraries that limit size (number of
334 gRNAs) and scope (number of targeted genes). Moreover, screen hits can be readily pursued
335 for downstream mechanistic analysis by individually cloning gRNAs used in the screen to easily

336 recreate strains outside of the pooled context, a clear benefit over random transposition
337 approaches such as Tn5. Additionally, generating pooled sub-libraries from screen hits enables
338 follow up validation at scale. Importantly, the ability to insert transposons with or without
339 promoters at the same genomic locus will allow researchers to disentangle the effects of Tn
340 insertion versus overexpression, simplifying hit interpretation. Further, combining CRISPRtOE
341 with existing gene perturbation approaches such as CRISPRi could enable screening for
342 overexpression suppressors of essential functions at the genome-scale.
343 Our proof of principle work demonstrating that genome-scale CRISPRtOE can identify
344 resistance genes in *E. coli* K-12 holds promise for extending this approach to clinically relevant
345 pathogens with the goal of improving diagnosis and treatment. Importantly, CRISPRtOE action
346 is similar to clinically relevant antibiotic resistance mechanisms, such as IS element
347 transposition and overexpression of downstream resistance genes[56]. CRISPRtOE may also be
348 valuable for optimization of strains for industrial use. Industrial strain optimization often occurs
349 through loss of function[57] or directed evolution experiments[58], followed up by plasmid-based
350 overexpression of mutated pathways. CRISPRtOE streamlines this process in non-model
351 bacteria, particularly by enabling recreation of optimized strain features in different genetic
352 backgrounds by targeted transposition. Finally, CRISPRtOE-optimized strains may be
353 immediately useful in production, as CRISPRtOE as leaves no heterologously expressed *cas*
354 genes in the recipient strain. Such optimization experiments are currently underway.
355 CRISPRtOE is not without caveats and there may be scenarios in which it is
356 outperformed by other overexpression or gene manipulation strategies. CRISPRtOE and other
357 engineering approaches that insert promoters will alter expression of downstream genes in
358 operons, a phenomenon known as “polarity.” Polar effects could complicate, but not necessarily
359 preclude identification of gene-level CRISPRtOE phenotypes. Our view is that expression of
360 downstream genes is often advantageous due to fact that protein complexes are often found in
361 operons (e.g., efflux pump subunits). We expect that “No promoter” CRISPRtOE libraries will
362 largely allow for disambiguation of insertion versus overexpression phenotypes, but there may
363 be rare instances in which the combination of insertion and overexpression causes an
364 unexpected genetic interaction because operons contain functionally related genes. In this
365 scenario, Dub-seq or promoter recombineering strategies would be advantageous, as Dub-seq
366 expresses genes *in trans* and recombineering can be used to introduce more subtle *cis*
367 mutations that could avoid perturbing upstream genes. Dub-seq can also introduce
368 heterologous DNA from other species for phenotyping[14], something CRISPRtOE is not designed
369 to accomplish.

370

371 # Methods

372 **Strains and growth conditions.** Strains are listed in Table S1. Growth and antibiotic selection
373 conditions are also summarized in Table S6. *Escherichia coli*, *Acinetobacter baumannii*,
374 *Enterobacter cloacae*, *Klebsiella pneumoniae,* and *Pseudomonas aeruginosa* were grown in LB
375 broth, Lennox (BD240230) at 37°C (or 30°C for CRISPR-guided transposition) in a flask with
376 shaking at 250 rpm, in a culture tube on a roller drum, in a 96 well deepwell plate with shaking
377 at 900 rpm, or in a Tecan Sunrise plate reader shaking with OD600 measurements every 15
378 min. *Pseudomonas putida* and *Shewanella oneidensis* were grown in LB in a culture tube on a
379 roller drum or in a 96 well deepwell plate with shaking at 900 rpm at 30°C. *Zymomonas mobilis*
380 was grown in RMG medium (10g yeast extract and 2g KH_2PO_4 monobasic/liter with 2% glucose
381 added after autoclaving) at 30°C statically in a culture tube or deepwell plate. *E. coli* was grown
382 in Mueller Hinton Broth (MHB, BD 275730) for antibiotic minimal inhibitory concentration (MIC)
383 assays. Media was solidified with 1.5-2% agar for growth on plates. Antibiotics were added
384 when necessary: *E. coli* (100 µg/ml carbenicillin (carb), 30 µg/ml kanamycin (kan), or 50 µg/ml
385 spectinomycin (spt)), *A. baumannii* (60 µg/ml kan or 100 µg/ml apramycin (apr)), *E. cloacae* (30
386 µg/ml kan or 50 µg/ml spt), *K. pneumoniae* (60 µg/ml kan or 50 µg/ml spt), *P. aeruginosa* (30
387 µg/ml gentamicin (gen) or 1 mg/ml kan), *P. putida* (150 µg/ml apr or 60 µg/ml kan), *S.*
388 *oneidensis* (60 µg/ml kan or 30 µg/ml gen), and *Z. mobilis* (200 µg/ml gen or 100 µg/ml spt).
389 Diaminopimelic acid (DAP) was added at 300 µM to support growth of *dap- E. coli* strains.
390 Strains were preserved in 15% glycerol at -80°C.

391

392 **General molecular biology techniques.** Plasmids are listed in Table S2. Oligonucleotides are
393 listed in Table S3. *pir*-dependent plasmids were propagated in *E. coli* strain BW25141
394 (sJMP146) or its derivative sJMP3053. Plasmids were purified using the GeneJet Plasmid
395 Miniprep kit (Thermo K0503), the QIAprep Spin Miniprep Kit (Qiagen 27106), or the Purelink
396 HiPure Plasmid Midiprep kit (Invitrogen K210005). Plasmids were digested with restriction
397 enzymes from New England Biolabs (NEB, Ipswich, MA). Ligations used T4 DNA ligase (NEB
398 M0202) and fragment assembly used NEBuilder Hifi (NEB E2621). Genomic DNA was extracted
399 with the DNeasy Blood & Tissue Kit (Qiagen 69504) or the GeneJet genomic DNA purification
400 kit (Thermo K0721). DNA fragments were amplified by PCR using Q5 DNA polymerase (NEB
401 M0491, for cloning) or One*Taq* DNA Polymerase (NEB M0480, for analysis). PCR products
402 were spin-purified using the Monarch PCR & DNA Cleanup Kit (NEB T1030) or the DNA Clean

403 & Concentrator-5 kit (Zymo Research, Irvine, CA, D4013). Reactions were purified with 1.8X
404 Mag-Bind TotalPure NGS magnetic beads (Omega) on a magnetic rack (Alpaqua). DNA was
405 quantified spectrophometrically using a NanoDrop Lite or fluorometrically using a Qubit with the
406 HS or BR DNA kit (Thermo). Plasmids were transformed into electrocompetent *E. coli* cells
407 using a 0.1 cm cuvette (Fisher FB101) and a BioRad Gene Pulser Xcell on the Bacterial 1 *E.*
408 *coli* preset protocol (25 µF, 200 ohm, 1800 V) as described in detail previously[59].
409 Oligonucleotides were synthesized by Integrated DNA Technologies (Coralville, IA) or Agilent
410 (SurePrint Oligonucleotide library) (Santa Clara, CA). Sequencing was performed by Functional
411 Biosciences (Madison, WI), Plasmidsaurus (Eugene, OR), Azenta (South Plainfield, NJ), or the
412 University of Wisconsin-Madison Biotechnology Center Next Generation Sequencing Core
413 (UWBC NGS core, Madison, WI).
414
415 ***E. coli* Δ*lac* strain construction.** An *E. coli* MG1655 strain with a *lac* operon deletion (Δ*lac*,
416 Lac$^-$) was constructed by λ-Red-mediated recombination as previously described[60]. Briefly, *E.*
417 *coli* MG1655 (sJMP163) harboring the plasmid pSIM6 (pJMP170) encoding the λ-Red proteins
418 was transformed with a linear DNA fragment encoding an FRT-*kan*-FRT cassette which was
419 amplified by PCR from plasmid pJMP3099 using primers oJMP912 and oJMP913 which also
420 have 40 nt homology to the chromosomal insertion site**)** resulting in strain sJMP3267. The allele
421 was transferred from sJMP3267 to *E. coli* MG1655 (sJMP163) by P1–*vir*-mediated transduction,
422 as previously described[61], resulting in strain sJMP3269. The *kan* gene was removed by
423 transformation with plasmid pCP20 (pJMP3008), encoding a constitutively expressed FLP
424 recombinase, as previously described[62], resulting in strain sJMP3272. Full deletion of the *lac*
425 operon in sJMP3272 was confirmed by PCR with flanking primers (oJMP914 and oJMP915)
426 followed by Sanger sequencing.
427
428 **Construction of fluorescent reporters and insertion into the att_{Tn7} site on the bacterial**
429 **chromosome.** Fluorescent reporter cassettes are located in a Tn*7* transposon located on an
430 R6K ori (*pir* dependent) plasmid. The transposons were transferred to the att_{Tn7} site ~50 bp
431 downstream of *glmS* of a recipient bacterial chromosome by co-conjugation of the Tn*7*
432 transposon donor strain and a second donor strain harboring a plasmid expressing Tn*7*
433 transposase[63]. Donor strains encode conjugation machinery, encode *pir*, and are DAP
434 dependent. Briefly, a donor strain with the transposon plasmid, a second donor with the
435 transposase expression plasmid, and the recipient strain were resuspended from plates to an
436 OD_{600}=9 and mixed in equal proportions (100 µl each). Cells were harvested by centrifugation at

437 5000 rcf for 2 min (except *A. baumannii* at 9000 rcf) and placed on a nitrocellulose filter
438 (Millipore HAWP01300) on an LB plate (except *Z. mobilis* on RMG) and incubated at 30°C (*Z.*
439 *mobilis* and *P. putida*) or 37°C (all other organisms) for 2-18h. Cells from the filter were
440 resuspended in 300 µl media, serially diluted, and plated with antibiotic selection for the
441 transposon (see growth and selection conditions above) and without DAP to select against the
442 donor strains, and incubated at 30 or 37°C until colonies formed.
443 A transposon containing a GFP expression cassette was derived from a Mobile-CRISPRi
444 plasmid[59] by assembling the AscI-EcoRI fragment of pJMP2824 and annealed oligonucleotides
445 oJMP1420 and oJMP1421 to create pJMP6957. The GFP encoding gene of pJMP6957 was
446 replaced by an mScarlet-I encoding gene derived from Addgene plasmid 85069 (pJMP7001) to
447 create pJMP10180 which has an *mScarlet-I* cassette (BbsI sites removed and *mScarlet*
448 converted to *mScarlet-I*) with the T7A1 constitutive promoter in the Tn*7* transposon. A
449 promoterless *mScarlet-I* reporter with the CRISPRt *LZ1* protospacer was derived from
450 pJMP6957, pJMP10180, and synthetic DNA oJMP1599 to create pJMP10206 (see Table S2 for
451 details).
452
453 **Construction of CRISPRt/CRISPRtOE system.** The CRISPRt/CRISPRtOE donor plasmids
454 were derived from pSpinR (pSL1765)[21], Mobile-CRISPRi plasmids[63], and synthetic DNA.
455 Cloning details are located in Supplementary Table S2 for the individual plasmids. In summary,
456 (1) a functional antibiotic resistance cassette was added to the transposon (pJMP747) and the
457 BsaI cloning site in the gRNA cassette was altered (pJMP10009 and pJMP10011). A two
458 plasmid R6K ori (*pir*-dependent) system for selectable CRISPR-guided transposition was
459 created by combining (1) the TnsABC-TniQ-Cas876 expression cassette from pSpinR with the
460 amp^R, R6K ori, mobilizable backbone from Mobile-CRISPRi (pJMP2782) to create pCRISPRt-H
461 (pJMP10233) and (2) the transposon and guide RNA cassette from pJMP10011 with the same
462 backbone (from pJMP2782) to create pCt-T (pJMP10237 and derivatives) which was further
463 minimized, optimized, and altered by adding transcription terminators and moving the guide
464 RNA cassette inside the transposon to produce pCRISPRt-T-gent (pJMP10395) and pCRISPRt-
465 T-kan (pJMP10397). CRISPRtOE plasmids with either no promoter or various strength
466 promoters (pCtOE-noP, pCtOE-P_A, pCtOE-P_H, pCtOE-P_V) were derived from these plasmids by
467 inserting a transcription terminator and promoter cassette derived from synthetic DNA
468 (oJMP2000 plus oJMP2001-2004) into the above plasmids to produce plasmids oJMP10471-
469 10479. Apramycin resistant derivatives of some of these plasmids were created by digesting

470 pJMP10397 and pJMP10478 with XhoI and assembling with a piece of synthetic DNA
471 (oJMP1946) encoding an apramycin resistance gene.
472
473 **CRISPRtOE Guide Design.** Guide RNAs were designed using custom Python scripts, available
474 with usage notes at GitHub repositories: https://github.com/ryandward/CRISPRt_gRNA and
475 https://github.com/ryandward/seq_hunter. Initially, the *Escherichia coli* K-12 RefSeq genome
476 assembly, in GenBank file format, was downloaded from the NCBI database (Accession
477 Number: GCF_000005845.2), using the seq_hunter.py script. The CRISPRt_gRNA.py script
478 was employed to identify all genomic locations with a suitable "CN" PAM sequence.
479 Subsequently, potential spacers of 32 nucleotides in length were evaluated using awk, and ten
480 were selected based on the following criteria: 1) Unique occurrence in the genome, 2)
481 occurrence on the same strand as the downstream gene, 3) at least 95 nucleotides upstream
482 from the gene annotation**.**
483
484 **CRISPRt/CRISPRtOE individual guide and guide library construction.** Guide sequences
485 were ligated into the BsaI-cloning site of the pCRISPRt-T/pCtOE plasmids. For cloning
486 individual spacer sequences, two 36-nucleotide (nt) oligonucleotides (oligos) were annealed so
487 that they encode the desired sequence flanked by sticky ends compatible to the vector BsaI site
488 whereas for cloning pooled libraries, DNA fragments encoding spacers were amplified from a
489 pool of oligos and digested with BsaI prior to ligation.
490 To prepare the pCRISPRt-T/pCtOE vectors for cloning, plasmid DNA was extracted from a 100
491 ml culture using a midiprep kit, 2-10 µg plasmid DNA was digested with BsaI-HF-v2 (NEB
492 R3733) in a 100 µl reaction for 4 h at 37°C and then spin-purified.
493 For cloning individual guides, pairs of oligonucleotides (2 µM each) were mixed in a 50 µl total
494 volume of 1X NEB CutSmart buffer, heated at 95°C, 5 min and then cooled to room temperature
495 ~20 min to anneal, and then diluted 1:40 in dH_2O prior to ligation. Ligation reactions (10 µl)
496 contained 1X T4 DNA ligase buffer (NEB), additional DTT (10 mM final) and ATP (0.1 mM final),
497 and 0.5 µl T4 DNA ligase in addition to 50 ng BsaI-digested/spin-purified vector and 2 µl of 1:40
498 diluted annealed oligos. Ligations were incubated at 25°C for 2 h and ligase was heat
499 inactivated for 20 min at 65°C. 1-2 µl ligation was used for electroporation into 50 µl *E. coli*
500 strain BW25141 (sJMP146). Transformations were serially diluted and plated with selection on
501 carb to obtain isolated colonies. After confirmation of sequence, individual plasmids were
502 transformed into *E. coli* mating strain WM6026 (sJMP424 or sJMP3257) with selection on carb
503 and DAP.

504 For cloning pooled libraries, fragments were amplified from 90 nt pooled oligos (IDT oPools or
505 Agilent SurePrint pools) using the following conditions per 100 µl reaction (reaction size was
506 adjusted ~100-600 µl depending on size of library): 20 µl Q5 buffer, 3 µl GC enhancer, 2 µl
507 10mM each dNTPs, 5 µl each 10 µM forward and reverse primers, 2 µl 10 nM pooled oligo
508 library, 1 µl Q5 DNA polymerase, and 186 µl H_2O with the following thermocycling parameters:
509 98°C, 30s; 15-19 cycles of: 98°C, 15s; 56°C, 15s; 72°C, 15s; 72°C, 10 min; 10°C, hold (cycles
510 were adjusted to obtain sufficient PCR product without overamplifying/biasing the library). PCR
511 products (90 bp) were spin-purified and 300 ng was digested with BsaI-HF-v2 (NEB R3733) in a
512 100 µl reaction for 2 h at 37°C (no heat kill, reaction size was adjusted proportionally depending
513 on the size of the library). Size and digestion of PCR products were confirmed on a 4% agarose
514 E-Gel (Thermo). The BsaI-digested PCR product without further purification (3ng/µl) was ligated
515 into BsaI-digested, spin-purified plasmid as described above except 10 µl of the digested PCR
516 product was ligated with 500 ng cut plasmid in a 100 µl reaction and ligations were incubated at
517 16°C for 14 h. Library ligations were purified by spot dialysis on a nitrocellulose filter (Millipore
518 VSWP02500) against 0.1 mM Tris, pH 8 buffer for 20 min prior to transformation by
519 electroporation into *E. coli* mating strain WM6026 (sJMP424 or sJMP3257). To obtain sufficient
520 transformants for large libraries, electrocompetent cells were made 5X more concentrated in the
521 final step of the preparation[59] and multiple transformations were carried out depending on the
522 size of the library. Transformations were plated with selection on LB with carb and DAP at a
523 density of ~30,000-50,000 colonies/150 mm petri plate. Cells (>30X more colonies the number
524 of guides, e.g. >1.35 million CFU for the 45,000 guide libraries) were scraped from plates and
525 resuspended in LB + 15% glycerol, density was adjusted to OD_{600}=9, and aliquots were frozen
526 at -80°C.
527
528 **Transfer of the CRISPRt/CRISPRtOE system to the bacterial chromosome.** CRISPRt and
529 CRISPRtOE strains were constructed by triparental mating of two *E. coli* donor strains—one
530 with the pCRISPRt-H plasmid encoding Cas678-TniQ-TnsABC and another with the pCRISPRt-
531 T or pCtOE plasmid containing the transposon with the guide RNA and antibiotic resistance—
532 and a recipient strain. See Supplementary Table S6 for a summary of growth media and
533 conditions and antibiotic concentrations. All conjugations and selection post-conjugation were
534 carried out at 30°C regardless of the normal incubation temperature for the organism. Isolated
535 donor and recipient strains were struck out on plates with the appropriate media and antibiotic (if
536 relevant) concentrations. Colonies were resuspended from plates into the growth medium used
537 for the recipient to a density of OD_{600}=9. Equal amounts of donors and recipient were mixed

538 together (along with the appropriate no recipient, no CRISPRt-H donor, or no CRISPRt-T donor
539 controls), cells were pelleted by centrifugation at 5000 x *g* (except *A. baumannii* at 9000 x *g*),
540 placed on a nitrocellulose filter on an LB plate (except an RMG plate for *Z. mobilis*), and
541 incubated 12-18 h at 30°C. Cells from the filter were resuspended in 300 µl media, serially
542 diluted, and plated with antibiotic selection for the transposon (see growth and selection
543 conditions above) and without DAP to select against the donor strains, and incubated at 30°C
544 until colonies formed (1-3 days). A typical mating was 100 µl each strain and plating 100 µl
545 undiluted, and 10^{-1} through 10^{-4} dilutions to obtain isolated colonies. For library construction,
546 conjugations were scaled up and plated with selection at a density of ~30,000-50,000
547 colonies/150 mm petri plate. Cells (>30X more colonies the number of guides, e.g. >1.35 million
548 CFU for the 45,000 guide libraries) were scraped from plates and resuspended in LB + 15%
549 glycerol, density was adjusted to OD_{600}=10-15, and aliquots were frozen at -80°C.
550
551 **Analysis of phenotype of *E. coli lacZ* and *gfp*-targeting CRISPRt.**
552 For *gfp* targeted CRISPRt, fluorescence level (GFP) of 80 individual colonies was determined.
553 Cultures were grown in 300 µl media in 96 well deepwell plates from a single colony to
554 saturation. Cells were centrifuged at 4,000 x *g* for 10 min and cell pellets were resuspended in
555 300 µl 1X PBS. 150 µl was transferred to a 96-well black, clear bottom microplate (Corning
556 3631) and cell density (OD_{600}) and fluorescence (excitation 475 nm, emission 510 nm) were
557 measured in a fluorescence microplate reader (Tecan Infinite Mplex). Fluorescence values were
558 normalized to cell density.
559 For *lacZ* targeted CRISPRt, the color of 80 individual colonies was determined by patching on
560 LB agar plates containing X-gal (20 µg/ml). Blue indicates the presence of an intact *lacZ* due to
561 metabolism of the X-gal by LacZ (betagalactosidase) and white indicates disruption of *lacZ*.
562
563 **Analysis of individual CRISPRtOE isolates from various Proteobacteria.**
564 <u>Phenotype determination</u>. Fluorescence levels (mScarlet-I) of 12 CRISPRtOE isolates of all 8
565 species were determined. Cultures of isolates were grown in 300 µl media in 96 well deepwell
566 plates from a single colony to saturation. Cultures were serially diluted to 1:10,000 (1:100 twice)
567 into fresh media and grown again to saturation (~13 doublings). Cells were centrifuged at 4,000
568 x *g* for 10 min. Cell pellets were resuspended in 300µl 1X PBS and 150 µl was transferred to a
569 96-well black, clear bottom microplate (Corning 3631). Cell density (OD600) and fluorescence
570 (excitation 584 nm, emission 607 nms) were measured in a fluorescence microplate reader

571 (Tecan Infinite Mplex). Fluorescence values were normalized to cell density. The assay was
572 repeated three times for *E. coli* and *Z. mobilis* and twice for all other strains.
573
574 Genotype determination. Insertion positions of 12 CRISPRtOE isolates of all 8 species were
575 determined. Cultures of isolates were grown in 300 µl media in 96 well deepwell plates, serially
576 diluted 1:100 in dH_2O, heated to 90°C for 3 min prior to use as a template for PCR. Fragments
577 (~2000 bp) were amplified by PCR with a forward primer in the transposon (oJMP490) and a set
578 of indexed (4 nt barcode) reverse primers in the *mScarlet-I* coding sequence (oJMP2118-2129)
579 in a 25 µl reaction containing: 5 µl OneTaq buffer, 0.5 µl 10mM each dNTPs, 0.5 µl each 10 µM
580 forward and reverse primers, 2 µl diluted culture, 0.25 µl OneTaq DNA polymerase, and 16.25 µl
581 H_2O with the following touchdown PCR program: 94°C, 3 min then 10 cycles of 94°C, 30s,
582 65°C, 30s (-1°C/cycle), 68°C, 2.5 min, then 25 cycles of 94°C, 30s, 55°C, 30s, 68°C, 2.5 min,
583 then 68°C, 5 min in a BioRad T100 thermalcycler. Sets of indexed PCRs for each organism
584 were pooled, spin purified and sequenced by Oxford nanopore long read amplicon sequencing
585 by Plasmidsaurus. Sequencing data was demultiplexed using a custom Python script
586 (SplitSamplesSeq.py) and insertion position relative to the *mScarlet-I* ATG start codon was
587 determined.
588
589 **CRISPRtOE library growth experiments.**
590 Competition experiment growth. The *E. coli* CRISPRtOE *murA* and *folA* libraries were mixed in
591 equal volume with the LP-*lacZ* library: 50 µl frozen stock (OD_{600} = 10) of each library (*murA* +
592 LP-*lacZ* and *folA* + LP-*lacZ*) into 100 ml LB (starting OD_{600} = 0.01) in a 500 ml flask and
593 incubated shaking at 37°C until OD_{600} = 0.2 (~2.5 h) (timepoint = T0) to revive the cells. These
594 cultures were diluted to OD_{600} = 0.02 into 4 ml LB plus antibiotic fosfomycin (0.4 µg/ml, for the
595 *murA* + LP-*lacZ* libraries) or trimethoprim (0.1 µg/ml, for the *folA* + LP-*lacZ* libraries) or no
596 antibiotic control in 14 ml snap cap culture tubes (Corning 352059) in duplicate and incubated
597 with shaking for 18 h at 37°C (T1). These cultures were serially diluted back to OD_{600} = 0.01 into
598 fresh tubes containing the same media and incubated again with shaking for 18 h at 37°C (T2)
599 for a total of ~10-15 doublings. Cells were pelleted from 15 ml of culture in duplicate at each
600 time point T0 and 1ml of culture at timepoints T1 and T2 and stored at -20°C.
601
602 Whole genome experiment growth. The *E. coli* CRISPRtOE whole genome libraries with no
603 promoter (sJMP10704) or promoter H (sJMP10705) were revived by dilution of 100 µl frozen
604 stock (OD_{600} = 15) into 100 ml LB (starting OD_{600} = 0.015) and incubation in 500 ml flasks

605 shaking at 37°C until OD_{600} = 0.2 (~2.5 h) (timepoint = T0). These cultures were diluted to OD_{600}
606 = 0.02 into 4 ml LB plus antibiotic trimethoprim (0.1 µg/ml) or no antibiotic control in 14 ml snap
607 cap culture tubes (Corning 352059) in duplicate and incubated with shaking for 18 h at 37°C
608 (T1). These cultures were serially diluted back to OD_{600} = 0.01 into fresh tubes containing the
609 same media and incubated again with shaking for 18 h at 37°C (T2) for a total of ~10-15
610 doublings. Cells were pelleted from 15 ml of culture in duplicate at time point T0 and 1ml of
611 culture at timepoints T1 and T2 and stored at -20°C.
612
613 **Analysis of individual CRISPRtOE isolates from library competition experiment.**
614 Insertion positions of 8 CRISPRtOE isolates from the *folA* and *murA* libraries were determined.
615 Cultures of isolates were grown in 3 ml media from an isolated colony, serially diluted 1:100 in
616 dH_2O, heated to 90°C for 3 min prior to use as a template for PCR. Fragments (~600 bp) were
617 amplified by PCR with a forward primer in the transposon (oJMP61) and a reverse primer in the
618 *folA* or *murA* coding sequence (oJMP2349 and oJMP2348, respectively) in a 50 µl reaction
619 containing: 10 µl OneTaq buffer, 1.0 µl 10mM each dNTPs, 1.0 µl each 10 µM forward and
620 reverse primers, 2 µl diluted culture, 0.5 µl OneTaq DNA polymerase, and 16.25 µl H_2O with the
621 following touchdown PCR program: 94°C, 3 min then 10 cycles of 94°C, 30s, 65°C, 30s (-
622 1°C/cycle), 68°C, 1 min, then 25 cycles of 94°C, 30s, 55°C, 30s, 68°C, 1 min, then 68°C, 5 min
623 in a BioRad T100 thermalcycler. PCR products were spin-purified and Sanger sequenced to
624 determine the transposon insertion position relative to the *mScarlet-I* ATG start codon.
625
626 **Tnseq analysis of CRISPRt/CRISPRtOE constructs.** TnSeq protocol was adapted from
627 Klompe et al[31]. Genomic DNA (gDNA) was extracted from the equivalent of 1 ml of cells at
628 OD_{600}=3 (~$2x10^9$ cells) either resuspended from a plate or from liquid culture and was further
629 purified by spot dialysis on a nitrocellulose filter (Millipore VSWP02500) against 0.1 mM Tris, pH
630 8 buffer for 20 min. 1 µg gDNA was digested with 4U MmeI (NEB) in a 50 µl reaction at 37°C, 12
631 hrs and heat inactivated at 65°C, 20 min. The digest was purified using 1.8X magnetic beads
632 (Omega) following the manufacturer's protocol, eluting in 20 µl 10 mM Tris, pH 8.0. Adapter
633 oligos oJMP1995 and P-oJMP1996 (phosphorylated) were annealed by mixing equal volume of
634 100µM oligos in 10mM Tris, pH8 (50 µM each), heating to 95°C, 5 min followed by cooling to RT
635 ~15 min, and diluted 1:10 (5 µM each) for use. Annealed oligos were ligated onto MmeI-
636 digested DNA in a 20 µl reaction with 2 µl 10X T4 ligase buffer, 2 µl 100 mM DTT, 2 µl 1 mM
637 ATP, 12 µl purified MmeI-digested gDNA (50 ng/µl, 600 ng total), 1 µl 5 µM annealed adapter
638 oligos (250 nM final) and 1 µl T4 DNA ligase. Ligations were incubated 14 h at 16°C and the

639 enzyme was heat-inactivated for 20 min at 65°C. Ligations were purified using 1.8X magnetic
640 beads, eluting in 22 µl 10 mM Tris, pH 8. Fragments were amplified by PCR with primers
641 containing partial adapters for index PCR with Illumina TruSeq adapters in a 100µl reaction
642 containing: 20 µl 5X Q5 buffer, 3 µl GC enhancer, 2 µl 10 mM each dNTPs, 5 µl each forward
643 primer (oJMP1997) and reverse primer (oJMP1998 or indexed primers oJMP2022-2033), 10 µl
644 purified ligation, 1 µl Q5 DNA polymerase, and 54 µl dH_2O with the following program: 98°C, 30s
645 then 18-20 cycles of 98°C, 15s, 66°C, 15s, 72°C, 15s, then 72°C, 10 min in a BioRad C1000
646 thermal cycler. PCR products were spin-purifed (eluted in 15 µl) and quantified fluorometrically.
647 Samples were sequenced by the UWBC NGS Core facility or Azenta Amplicon-EZ service.
648 Briefly, PCR products were amplified with nested primers containing i5 and i7 indexes and
649 Illumina TruSeq adapters followed by bead cleanup, quantification, pooling and running on a
650 NovaSeq X Plus (150 bp paired end reads) or MiSeq (250 bp paired end reads). Sequencing
651 analysis of the initial CRISPRt or CRISPRtOE plasmid libraries from which the strain libraries
652 were prepared was by amplification with oJMP2011 and oJMP1998 (or barcoded version of
653 oJMP1998: oJMP2022-2033), followed by spin purification and Illumina sequencing.
654
655 **Analysis of *E. coli mScarlet-I*-targeting CRISPRt libraries.**
656 Two plasmid libraries (pJMP10505 and pJMP10506) were constructed (gen^R and kan^R) and
657 used to create CRISPRtOE libraries (sJMP10519, 10520, 10594, 10595, and 10637-10640) in
658 each of four *E. coli mScarlet-I* reporter strains (sJMP10205, 10269, 10630, 10633). Plasmid
659 DNA from pJMP10505 and pJMP10506 was amplified with oJMP2011 and oJMP1998. gDNA
660 from (sJMP10519, 10520, 10594, 10595, and 10637-10640) was processed by TnSeq as
661 detailed above with oJMP1997 and oJMP2022-2033. Sequencing data was demultiplexed using
662 SplitSamplesSeq.py and guides were quantified using seal.sh from bbmap.
663
664 **MIC assays.** The minimal inhibitory concentration (MIC) of *E. coli folA* and *murA* CRISPRtOE
665 isolates was determined by either growth in a microtiter plate or by disc diffusion assays,
666 respectively. For the broth microdilution assay, CRISPRtOE isolates and WT controls were
667 grown to saturation from an isolated colony and serially diluted to OD600 = 0.003) and the
668 CRISPRtOE library was diluted from a glycerol stock to the same density. Trimethoprim was
669 serially diluted in DMSO at 1000X concentration and then diluted to 2X in MHB. *E. coli folA*
670 CRISPRtOE isolates, the *folA* CRISPRtOE library, a *lacZ* CRISPRtOE control, and WT cultures
671 and the media containing antibiotic were mixed in equal proportions and incubated 20 h shaking
672 at 37°C prior to cell density (OD_{600}) determination in a microplate reader. For the MIC strip

673 assays, *E. coli folA* or *murA* CRISPRtOE isolates, a *lacZ* CRISPRtOE control, and WT cultures
674 were diluted to OD_{600} = 0.3 and 300 µl was spread on a 100 mm MH agar plate and dried in a
675 laminar flow cabinet. When dry, MIC strips (Liofilchem, Italy; 920371 (TMP 0.002-32 mg/L) and
676 920791(FOS 0.064-1024 mg/L)) were applied to the plate and 10 µl serially diluted antibiotics
677 were applied to the discs. Plates were incubated at 37°C for 18 h. Broth microdilution assays
678 were repeated 3 times and MIC test strip assays twice.
679
680 **CRISPRtOE data processing and analysis.** All commands and scripts used for processing
681 and analysis of CRISPRtOE data can be found on GitHub
682 (https://github.com/GLBRC/CRISPRtOE_Analysis). FASTQ files were separated for each read
683 (R1 and R2), concatenated, and trimmed to remove transposon-specific sequences using
684 Cutadapt (v3.4)[64] using default parameters and sequences flanking the desired genome
685 sequence. The trimmed FASTQ files were aligned to the *E. coli* genome (NCBI RefSeq
686 Assembly ID GCF_000005845.2) using Bowtie2 (v2.4.4)[65] using default parameters for paired-
687 end alignment. The alignment SAM file for each sample was filtered using Samtools (v1.13)[66] to
688 remove unmapped reads (-F 8) and to remove reads that mapped to opposite strands (-F 0x2).
689 This resulted in paired end reads that aligned to the same DNA strand. BBMap (v38.32)[67] was
690 used to filter the SAM files to remove read pairs wherein at least one read is less than 2
691 nucleotides or greater than 50 nucleotides in order to identify specific transposon insertion sites
692 downstream of spacer sequences. A custom Python script (parsing_sam_for_hisogram.py) and
693 a custom Rscript (Histogram_CRISPRtOE.R) were used to parse the filtered SAM files and
694 construct histograms representing the distance between the spacer sequence and the
695 transposon insertion site.
696 The SAM files for each sample were further filtered to remove reads there were more than 100
697 nucleotides apart using the Picard tools (v2.20)[68] “FilterSamReads” function with default
698 parameters. This resulted in an aligned file where in the spacer sequence was located on the
699 same strand as the transposon insertion site and in the same location (within 100 nucleotides).
700 These filtered files were used for all further analyses. Samtools (v1.13)[66] was used to sort and
701 index these files and DeepTools (v3.5.1)[69] was used to construct BigWig files (normalized using
702 CPM) and Bed files for visualization. To identify the distance between the transposon insertion
703 site and the nearest gene downstream, the alignment file was filtered to include only reads < 25
704 nucleotides (those reads corresponding to the site of transposon insertion) using Samtools
705 (v1.13)[66] and a custom Python script (site_of_insertion.py) was used to generate a resulting
706 table of the location of transposon insertion sites. The table was converted to a Bed file using a

707 custom Python script (table_to_bed.py) and the BEDOPS (v2.4.41)[70] command "closest-
708 features" was used to identify the distance between transposon insertion site and the nearest
709 gene downstream. CRISPRtOE distance results from all samples were combined and a custom
710 Python script (make_table_for_histogram.py) was used to construct the input for R. To compare
711 CRISPRtOE insertion sites relative to genes to that of traditional Tn-seq, Tn-seq data from
712 Goodall *et al.*[71] (TL1 samples) were aligned to the same *E. coli* genome (NCBI RefSeq
713 Assembly ID GCF_000005845.2) using Bowtie2 (v2.4.4)[65] using default parameters and Bed
714 files were created using DeepTools (v3.5.1)[69] as described above. The Tn-seq data was
715 processed to identify the distance between transposon insertion and the gene downstream and
716 compared to CRISPRtOE distance as above. Data were visualized on the IGV Genome
717 Browser[72] and Circos plots were created using Proksee[73].
718 A custom Python script (counting_spacers.py) was used to determine the number of times each
719 spacer appeared in the filtered alignment file. Spacers were retained for analysis if they had a
720 count ≥5. Pairwise comparison of spacer counts in DMSO and TMP treatment samples was
721 performed using edgeR[74] and a custom Rscript (comparison_of_spacer_counts_edgeR.R). The
722 results were plotted using a custom Rscripts (plotting_scatter_plot.R, barplot_with_points.R,
723 scatter_plot_commands.R). For gene analysis, spacers for each gene were averaged and
724 genes were retained if they contained >2 spacers for further analysis.
725

726 ## Data availability

727 Sequencing data will be deposited at the Sequence Read Archive. All other data are available
728 upon request.
729

730 ## Code availability

731 Guide design script is available at https://github.com/ryandward/CRISPRt_gRNA. Analysis and
732 demultiplexing scripts are available at https://github.com/GLBRC/CRISPRtOE_Analysis.
733

734 ## References

735 1. Jost, M. *et al.* Combined CRISPRi/a-Based Chemical Genetic Screens Reveal that Rigosertib
736 Is a Microtubule-Destabilizing Agent. *Molecular Cell* **68**, 210-223.e6 (2017).
737 2. Kampmann, M. Elucidating drug targets and mechanisms of action by genetic screens in
738 mammalian cells. *Chem Commun (Camb)* **53**, 7162–7167 (2017).

739 3. Kampmann, M. CRISPRi and CRISPRa Screens in Mammalian Cells for Precision Biology
740 and Medicine. *ACS Chem Biol* **13**, 406–416 (2018).
741 4. Cámara, E., Lenitz, I. & Nygård, Y. A CRISPR activation and interference toolkit for industrial
742 Saccharomyces cerevisiae strain KE6-12. *Sci Rep* **10**, 14605 (2020).
743 5. Dominguez, A. A., Lim, W. A. & Qi, L. S. Beyond editing: repurposing CRISPR-Cas9 for
744 precision genome regulation and interrogation. *Nat Rev Mol Cell Biol* **17**, 5–15 (2016).
745 6. Jost, M. & Weissman, J. S. CRISPR Approaches to Small Molecule Target Identification. *ACS*
746 *Chem Biol* **13**, 366–375 (2018).
747 7. Lian, J., Schultz, C., Cao, M., HamediRad, M. & Zhao, H. Multi-functional genome-wide
748 CRISPR system for high throughput genotype-phenotype mapping. *Nat Commun* **10**, 5794
749 (2019).
750 8. Santiago, M. *et al.* A new platform for ultra-high density Staphylococcus aureus transposon
751 libraries. *BMC Genomics* **16**, 252 (2015).
752 9. Kitagawa, M. *et al.* Complete set of ORF clones of Escherichia coli ASKA library (a complete
753 set of E. coli K-12 ORF archive): unique resources for biological research. *DNA Res.* **12**,
754 291–299 (2005).
755 10. Tal, S. & Paulsson, J. Evaluating quantitative methods for measuring plasmid copy
756 numbers in single cells. *Plasmid* **67**, 167–173 (2012).
757 11. Freed, E. F. *et al.* Genome-Wide Tuning of Protein Expression Levels to Rapidly
758 Engineer Microbial Traits. *ACS Synth Biol* **4**, 1244–1253 (2015).
759 12. Warner, J. R., Reeder, P. J., Karimpour-Fard, A., Woodruff, L. B. A. & Gill, R. T. Rapid
760 profiling of a microbial genome using mixtures of barcoded oligonucleotides. *Nat Biotechnol*
761 **28**, 856–862 (2010).
762 13. Mutalik, V. K. *et al.* Dual-barcoded shotgun expression library sequencing for high-
763 throughput characterization of functional traits in bacteria. *Nat Commun* **10**, 308 (2019).
764 14. Huang, Y. Y. *et al.* Barcoded overexpression screens in gut Bacteroidales identify genes
765 with new roles in carbon utilization and stress resistance. 2022.10.10.511384 Preprint at
766 https://doi.org/10.1101/2022.10.10.511384 (2023).
767 15. Mali, P. *et al.* CAS9 transcriptional activators for target specificity screening and paired
768 nickases for cooperative genome engineering. *Nat Biotechnol* **31**, 833–838 (2013).
769 16. Lee, D. J., Minchin, S. D. & Busby, S. J. W. Activating transcription in bacteria. *Annu Rev*
770 *Microbiol* **66**, 125–152 (2012).

771 17. Bikard, D. *et al.* Programmable repression and activation of bacterial gene expression
772 using an engineered CRISPR-Cas system. *Nucl. Acids Res.* gkt520 (2013)
773 doi:10.1093/nar/gkt520.
774 18. Kiattisewee, C. *et al.* Expanding the Scope of Bacterial CRISPR Activation with PAM-
775 Flexible dCas9 Variants. *ACS Synth Biol* **11**, 4103–4112 (2022).
776 19. Ho, H.-I., Fang, J. R., Cheung, J. & Wang, H. H. Programmable CRISPR-Cas
777 transcriptional activation in bacteria. *Mol Syst Biol* **16**, e9427 (2020).
778 20. Peters, J. E., Makarova, K. S., Shmakov, S. & Koonin, E. V. Recruitment of CRISPR-Cas
779 systems by Tn7-like transposons. *PNAS* **114**, E7358–E7366 (2017).
780 21. Vo, P. L. H. *et al.* CRISPR RNA-guided integrases for high-efficiency, multiplexed
781 bacterial genome engineering. *Nat Biotechnol* **39**, 480–489 (2021).
782 22. Rubin, B. E. *et al.* Species- and site-specific genome editing in complex bacterial
783 communities. *Nat Microbiol* **7**, 34–47 (2022).
784 23. Chen, W. *et al.* Targeted genetic screening in bacteria with a Cas12k-guided
785 transposase. *Cell Rep* **36**, 109635 (2021).
786 24. Trujillo Rodríguez, L., Ellington, A. J., Reisch, C. R. & Chevrette, M. G. CRISPR-
787 Associated Transposase for Targeted Mutagenesis in Diverse Proteobacteria. *ACS Synth Biol*
788 **12**, 1989–2003 (2023).
789 25. Roberts, A., Nethery, M. A. & Barrangou, R. Functional characterization of diverse type I-
790 F CRISPR-associated transposons. *Nucleic Acids Res* **50**, 11670–11681 (2022).
791 26. Hsieh, S.-C. & Peters, J. E. Discovery and characterization of novel type I-D CRISPR-
792 guided transposons identified among diverse Tn7-like elements in cyanobacteria. *Nucleic*
793 *Acids Res* **51**, 765–782 (2023).
794 27. Walker, M. W. G., Klompe, S. E., Zhang, D. J. & Sternberg, S. H. Novel molecular
795 requirements for CRISPR RNA-guided transposition. *Nucleic Acids Res* **51**, 4519–4535
796 (2023).
797 28. Gelsinger, D. R. *et al.* Bacterial genome engineering using CRISPR RNA-guided
798 transposases. *bioRxiv* 2023.03.18.533263 (2023) doi:10.1101/2023.03.18.533263.
799 29. Hoffmann, F. T. *et al.* Selective TnsC recruitment enhances the fidelity of RNA-guided
800 transposition. *Nature* **609**, 384–393 (2022).
801 30. Halpin-Healy, T. S., Klompe, S. E., Sternberg, S. H. & Fernández, I. S. Structural basis of
802 DNA targeting by a transposon-encoded CRISPR-Cas system. *Nature* **577**, 271–274 (2020).
803 31. Klompe, S. E., Vo, P. L. H., Halpin-Healy, T. S. & Sternberg, S. H. Transposon-encoded
804 CRISPR–Cas systems direct RNA-guided DNA integration. *Nature* **571**, 219 (2019).

805 32. Garza Elizondo, A. M. & Chappell, J. Targeted Transcriptional Activation Using a
806 CRISPR-Associated Transposon System. *ACS Synth Biol* **13**, 328–336 (2024).
807 33. Petassi, M. T., Hsieh, S.-C. & Peters, J. E. Guide RNA Categorization Enables Target
808 Site Choice in Tn7-CRISPR-Cas Transposons. *Cell* **183**, 1757-1771.e18 (2020).
809 34. Banta, A. B., Enright, A. L., Siletti, C. & Peters, J. M. A High-efficacy CRISPRi System for
810 Gene Function Discovery in Zymomonas mobilis. *Appl. Environ. Microbiol.* (2020)
811 doi:10.1128/AEM.01621-20.
812 35. Hall, A. N. *et al.* Tools for Genetic Engineering and Gene Expression Control in
813 Novosphingobium aromaticivorans and Rhodobacter sphaeroides. *bioRxiv*
814 2023.08.25.554875 (2023) doi:10.1101/2023.08.25.554875.
815 36. Enright, A. L. *et al.* The genetics of aerotolerant growth in an alphaproteobacterium with
816 a naturally reduced genome. *mBio* e0148723 (2023) doi:10.1128/mbio.01487-23.
817 37. Rice, L. B. Federal funding for the study of antimicrobial resistance in nosocomial
818 pathogens: no ESKAPE. *J Infect Dis* **197**, 1079–1081 (2008).
819 38. Fenster, J. A. *et al.* Dynamic and single cell characterization of a CRISPR-interference
820 toolset in Pseudomonas putida KT2440 for β-ketoadipate production from p-coumarate.
821 *Metab Eng Commun* **15**, e00204 (2022).
822 39. Hau, H. H. & Gralnick, J. A. Ecology and biotechnology of the genus Shewanella. *Annu*
823 *Rev Microbiol* **61**, 237–258 (2007).
824 40. Prasad, N. K., Seiple, I. B., Cirz, R. T. & Rosenberg, O. S. Leaks in the Pipeline: a
825 Failure Analysis of Gram-Negative Antibiotic Development from 2010 to 2020. *Antimicrobial*
826 *Agents and Chemotherapy* **66**, e00054-22 (2022).
827 41. Peters, J. M. *et al.* A Comprehensive, CRISPR-based Functional Analysis of Essential
828 Genes in Bacteria. *Cell* **165**, 1493–1506 (2016).
829 42. Johnson, R. A. *et al.* Inhibition of Isoleucyl-tRNA Synthetase by the Hybrid Antibiotic
830 Thiomarinol. *J Am Chem Soc* **143**, 12003–12013 (2021).
831 43. Palmer, A. C. & Kishony, R. Opposing effects of target overexpression reveal drug
832 mechanisms. *Nat Commun* **5**, 4296 (2014).
833 44. Couce, A. *et al.* Genomewide overexpression screen for fosfomycin resistance in
834 Escherichia coli: MurA confers clinical resistance at low fitness cost. *Antimicrob Agents*
835 *Chemother* **56**, 2767–2769 (2012).
836 45. Ason, B. & Reznikoff, W. S. DNA sequence bias during Tn5 transposition. *J Mol Biol* **335**,
837 1213–1225 (2004).

838 46. Lee, J.-H., Lee, K.-L., Yeo, W.-S., Park, S.-J. & Roe, J.-H. SoxRS-mediated
839 lipopolysaccharide modification enhances resistance against multiple drugs in Escherichia
840 coli. *J Bacteriol* **191**, 4441–4450 (2009).
841 47. Griffith, K. L., Becker, S. M. & Wolf, R. E. Characterization of TetD as a transcriptional
842 activator of a subset of genes of the Escherichia coli SoxS/MarA/Rob regulon. *Mol Microbiol*
843 **56**, 1103–1117 (2005).
844 48. Seo, S. W., Kim, D., Szubin, R. & Palsson, B. O. Genome-wide Reconstruction of OxyR
845 and SoxRS Transcriptional Regulatory Networks under Oxidative Stress in Escherichia coli
846 K-12 MG1655. *Cell Rep* **12**, 1289–1299 (2015).
847 49. Jones, K. M., Guest, J. R. & Woods, D. D. Folic acid and the synthesis of methionine by
848 extracts of Escherichia coli. *Biochem J* **79**, 566–574 (1961).
849 50. Weissbach, H. & Brot, N. Regulation of methionine synthesis in Escherichia coli. *Mol*
850 *Microbiol* **5**, 1593–1597 (1991).
851 51. Saint-Girons, I. *et al.* Nucleotide sequence of metF, the E. coli structural gene for 5-10
852 methylene tetrahydrofolate reductase and of its control region. *Nucleic Acids Res* **11**, 6723–
853 6732 (1983).
854 52. Girgis, H. S., Hottes, A. K. & Tavazoie, S. Genetic architecture of intrinsic antibiotic
855 susceptibility. *PLoS One* **4**, e5629 (2009).
856 53. Nichols, R. J. *et al.* Phenotypic landscape of a bacterial cell. *Cell* **144**, 143–156 (2011).
857 54. Giladi, M., Altman-Price, N., Levin, I., Levy, L. & Mevarech, M. FolM, a new
858 chromosomally encoded dihydrofolate reductase in Escherichia coli. *J Bacteriol* **185**, 7015–
859 7018 (2003).
860 55. Rao, T. V. P. & Kuzminov, A. Exopolysaccharide defects cause hyper-thymineless death
861 in Escherichia coli via massive loss of chromosomal DNA and cell lysis. *Proc Natl Acad Sci U*
862 *S A* **117**, 33549–33560 (2020).
863 56. Partridge, S. R., Kwong, S. M., Firth, N. & Jensen, S. O. Mobile Genetic Elements
864 Associated with Antimicrobial Resistance. *Clin Microbiol Rev* **31**, e00088-17 (2018).
865 57. Martínez-García, E., Aparicio, T., de Lorenzo, V. & Nikel, P. I. New transposon tools
866 tailored for metabolic engineering of gram-negative microbial cell factories. *Front Bioeng*
867 *Biotechnol* **2**, 46 (2014).
868 58. Yang, Q. *et al.* Development and characterization of acidic-pH-tolerant mutants of
869 Zymomonas mobilis through adaptation and next-generation sequencing-based genome
870 resequencing and RNA-Seq. *Biotechnol Biofuels* **13**, 144 (2020).

871 59. Banta, A. B., Ward, R. D., Tran, J. S., Bacon, E. E. & Peters, J. M. Programmable Gene
872 Knockdown in Diverse Bacteria Using Mobile-CRISPRi. *Curr Protoc Microbiol* **59**, e130
873 (2020).
874 60. Sharan, S. K., Thomason, L. C., Kuznetsov, S. G. & Court, D. L. Recombineering: a
875 homologous recombination-based method of genetic engineering. *Nat Protoc* **4**, 206–223
876 (2009).
877 61. Thomason, L. C., Costantino, N. & Court, D. L. E. coli genome manipulation by P1
878 transduction. *Curr Protoc Mol Biol* **Chapter 1**, 1.17.1-1.17.8 (2007).
879 62. Cherepanov, P. P. & Wackernagel, W. Gene disruption in Escherichia coli: TcR and KmR
880 cassettes with the option of Flp-catalyzed excision of the antibiotic-resistance determinant.
881 *Gene* **158**, 9–14 (1995).
882 63. Peters, J. M. *et al.* Enabling genetic analysis of diverse bacteria with Mobile-CRISPRi.
883 *Nature Microbiology* **4**, 244–250 (2019).
884 64. Martin, M. Cutadapt removes adapter sequences from high-throughput sequencing
885 reads. *EMBnet.journal* **17**, 10–12 (2011).
886 65. Langmead, B. & Salzberg, S. L. Fast gapped-read alignment with Bowtie 2. *Nat Methods*
887 **9**, 357–359 (2012).
888 66. Li, H. *et al.* The Sequence Alignment/Map format and SAMtools. *Bioinformatics* **25**,
889 2078–2079 (2009).
890 67. Bushnell, B. BBMap: A Fast, Accurate, Splice-Aware Aligner. (2014).
891 68. Picard Tools - By Broad Institute. https://broadinstitute.github.io/picard/.
892 69. Ramírez, F. *et al.* deepTools2: a next generation web server for deep-sequencing data
893 analysis. *Nucleic Acids Res* **44**, W160-165 (2016).
894 70. Neph, S. *et al.* BEDOPS: high-performance genomic feature operations. *Bioinformatics*
895 **28**, 1919–1920 (2012).
896 71. Goodall, E. C. A. *et al.* The Essential Genome of Escherichia coli K-12. *mBio* **9**, e02096-
897 17 (2018).
898 72. Robinson, J. T., Thorvaldsdottir, H., Turner, D. & Mesirov, J. P. igv.js: an embeddable
899 JavaScript implementation of the Integrative Genomics Viewer (IGV). *Bioinformatics* **39**,
900 btac830 (2023).
901 73. Grant, J. R. *et al.* Proksee: in-depth characterization and visualization of bacterial
902 genomes. *Nucleic Acids Res* **51**, W484–W492 (2023).

903 74. Robinson, M. D., McCarthy, D. J. & Smyth, G. K. edgeR: a Bioconductor package for
904 differential expression analysis of digital gene expression data. *Bioinformatics* **26**, 139–140
905 (2010).
906

907 ## Acknowledgements

908 We thank members of the Peters lab and Michael Thomas for helpful discussions and Joshua
909 Hyman and the University of Wisconsin-Madison Biotechnology Center for technical assistance
910 with Illumina sequencing and Samuel Sternberg for plasmids. This work was supported by the
911 U.S. Department of Energy, Office of Science and Office of Biological and Environmental
912 Research, Great Lakes Bioenergy Research Center, under Award Number DE-SC0018409, and
913 by the National Institutes of Health under award number 1R35GM150487-01 to J.M.P.
914

915 ## Author contributions

916 A.B.B. and J.M.P. designed, performed, and interpreted the experiments and wrote the
917 manuscript with input from all authors. K.S.M. developed the data analysis pipeline and
918 performed data analysis. R.D.W. and M.P. developed code. R.A.C., C.C.F., and E.E.B
919 performed experiments.
920

921 ## Competing interests

922 The authors declare no competing interests.
923

924 ## Figure legends

925 **Fig. 1 A mobilizable, selectable, dual-plasmid system for CRISPR-guided transposition. a**
926 Schematic of a targeted transposition gene knockout (CRISPRt) and gene overexpression
927 (CRISPRtOE) system optimized for functional genomics. **b** Schematic of mechanism of *Vibrio*
928 *cholera* Type I-F CRISPR-associated transposon (VcCAST) system[20,21]. **c** Schematic of strain
929 construction using the CRISPRt targeted transposition system. Plasmids have pir-dependent
930 origins of replication preventing replication in the bacterial recipient. One plasmid encodes the
931 minimal Type I-F CRISPR-Cas (Cas678) and Tn7-like transposase (TnsABC and TniQ)
932 machinery, and a second plasmid contains a transposon carrying the guide RNA and antibiotic
933 resistance expression cassettes (see Fig S1 for details). These plasmids are transferred by co-
934 conjugation to a recipient bacterium by *E. coli* donor strains with a chromosomal copy of the
935 RP4 transfer machinery. Inside the recipient cell, the transposon (flanked in yellow) is inserted

936 onto the chromosome at a site determined by the sequence of the guide RNA. Selection on
937 antibiotic plates lacking diaminopimelic acid (DAP) selects for transconjugants and against the
938 *E. coli* donor strains. **d** Specificity of CRISPRt disruption of *gfp* and *lacZ* in *E. coli* measured by
939 Tnseq. Mapping of location of transposon insertion sites to the *E. coli* genome after CRISPRt
940 targeted transposition with *gfp1* guide (226,671 reads) or *LZ1* guide (216,801 reads). **e** Insertion
941 position (bp downstream of protospacer) frequency of CRISPRt disruption of *gfp* and *lacZ* in *E.*
942 *coli* (RL orientation). Percentage of on-target, RL orientation insertions for all positions with >
943 0.01%.
944
945 **Fig. 2 Transcription impacts efficacy of CRISPRt guides. a** Schematic of guides in pooled
946 *mScarlet-I* disruption experiment. Twenty-three guides matching protospacers located on top
947 (T1-24) or bottom (B1-24) strand of the mScarlet-I encoding gene with a range of CN guides
948 (see Table S4 for details). **b** Relative efficacy of CRISPRt *mScarlet-I* guides in a pooled screen
949 targeting *mScarlet-I* expressed from a transposon in the att_{Tn7} site on the *E. coli* chromosome.
950 Relative efficacy is expressed as the $\log_2$-fold change of the frequency in the CRISPRt libraries
951 (sJMP10519 and sJMP10520) vs. the frequency in the original plasmid construct libraries
952 (sJMP10505 and sJMP10506). Average and standard deviation of two separate CRISPRt
953 libraries (gentamicin^R and kanamycin^R) containing all 46 guides. **c** Absolute transposition
954 efficiency of 3 individual CRISPRt guides (T03, T09, T21) targeting *mScarlet-I* cassettes in the
955 *E. coli* att_{Tn7} site either with a promoter (+ transcription) or without a promoter (- transcription)
956 measured by plating efficiency with and without selection (+/- kanamycin) in triplicate. Error
957 represents the average of n=3 assays, * indicates $p<0.05$, two-tailed t-test.
958
959 **Fig. 3 Tunable overexpression of chromosomally located genes using CRISPRtOE. a**
960 Schematic of CRISPRtOE targeted overexpression system. The chromosomal target is an
961 *mScarlet-I* gene preceded by a 'Landing Pad' (LP) with no promoter, a PAM, and the *LZ1*
962 protospacer (see Fig S5a). The CRISPRtOE construct has a transposon carrying guide RNA
963 and antibiotic resistance expression cassettes and an outward facing promoter (see
964 Supplementary Fig. S5b). Co-conjugation of strains carrying the CRISPRtOE construct and the
965 CRISPRt-H plasmid (harboring the VcCAST machinery) with a promoterless *mScarlet-I* reporter
966 recipient strain results in a CRISPRtOE strain. **b** mScarlet-I fluorescence analysis of *E. coli*
967 CRISPRtOE isolates (no promoter or synthetic promoters A, V, and H) compared to the parent
968 (promoterless *mScarlet-I*) strain. **c** Fold effect of CRISPRtOE mScarlet-I overexpression using
969 Promoter H in eight Alpha- and Gammaprotebacteria (*E. coli* (*Eco*), *Enterobacter cloacae* (*Ecl*),

970 *Klebsiella pneumoniae* (*Kpn*), *Acinetobacter baumannii* (*Aba*), *Pseudomonas aeruginosa* (*Pae*),
971 *Pseudomonas putida* (*Ppu*), *Zymomonas mobilis* (*Zmo*), and *Shewanella oneidensis* (*Son*)).
972 CRISPRtOE transposon insertion position and fluorescence measurements were determined for
973 twelve isolates. Fluorescence measurements were normalized to cell density (OD_{600}). Values
974 are shown for isolates with on-target, RL orientation CRISPRtOE insertions and fold changes for
975 on-target and RL orientation CRISPRtOE isolates compared to a strain with promoterless
976 *mScarlet-I* (see Table S8 for details). Error is expressed for the median value of 8-12 isolates in
977 n=3 (*Eco* and *Zmo*) or n=2 (*Ecl*, *Kpn*, *Aba*, *Pae*, *Ppu*, and *Son*) assays.
978
979 **Fig. 4 CRISPRtOE informs antibiotic mode of action. a** Schematic of CRISPRtOE
980 competitive growth assay. A pooled CRISPRtOE strain library is constructed by amplification of
981 spacer sequences from a pooled oligo library and transfer onto the chromosome of a recipient
982 strain. Insertion of the CRISPRtOE transposon is either upstream of genes of interest or within a
983 control gene (e.g. *lacZ*) in *E. coli*. A CRISPRtOE pooled library screen is conducted by culturing
984 a CRISPRtOE pooled library and control library for multiple generations in the presence or
985 absence of a chemical or condition of interest. The change in the composition of the pooled
986 library before and after treatment is measured by amplification and NGS sequencing of the
987 spacer sequences. **b** CRISPRtOE pooled library screen. Fitness of pooled strains
988 overexpressing *folA* compared to the *lacZ* control strains in the presence of trimethoprim (TMP).
989 **c** MIC broth microdilution assay of individual CRISPRtOE *folA* strains compared to WT, a
990 CRISPRtOE *lacZ* isolate, and the CRISPRtOE *folA* pooled library in the presence of TMP (0.04-
991 20 μg/ml). Error is expressed for 3 separate assays.
992
993 **Fig. 5 Genome-scale CRISPRtOE. a** Genome plot showing positions of CRISPRtOE insertions
994 in TMP-treated cells. Data are scaled to the maximum number of counts. **b** Positions of
995 CRISPRtOE insertions upstream of all genes in the genome. Insertion site distance d was
996 calculated based on the distance in bp from the 3′ end of the Tn to the 5′ end of the gene. **c**
997 CRISPRtOE insertions into the *lac* locus. The scale is capped at 20 reads for visual clarity. **d**
998 Volcano plot of gRNA spacer counts in TMP vs DMSO control. **e** Top positive gene hits in TMP
999 treatment. Genes must have at least a 4-fold change in the promoter H data and show a 4-fold
1000 difference in a comparison between promoter H and no promoter to be considered. Error bars
1001 represent standard deviation (SD).
1002

1003 **Fig. S1 Details of CRISPRt plasmids and *E. coli* GFP reporter strain. a** Plasmid maps of
1004 CRISPRt-H helper and CRISPRt-T transposon plasmids. Both plasmids in the dual plasmid
1005 system have backbones with an R6K pir-dependent replication origin, an ampicillan resistance
1006 cassette, and conjugative transfer origin. The CRISPRt-H helper plasmid has expression
1007 cassettes for the minimal Vch CRISPR (Cas678) and Transposase (TnsABC, TniQ) machinery
1008 derived from pSpin-R[21]. The CRISPRt-T transposon plasmid encodes a modified VchINT
1009 transposon derived from pSpin-R[21] which includes a guide RNA expression cassette with a
1010 modified BsaI cloning site and an antibiotic expression cassette and transcription terminators
1011 derived from CRISPRi plasmids[63]. The antibiotic resistance cassette is flanked by XhoI sites to
1012 facilitate modification, three variants are shown. **b** Sequence of CRISPRt targeted transposition
1013 system guide RNA expression cassette including the BsaI cloning site for new guide RNAs. **c**
1014 Position of the P_{veg}-*sfgfp* expression cassette inserted between *yjaA* and *yjaB*. on the *E. coli*
1015 chromosome.
1016
1017 **Fig. S2 CRISPRt disruption efficiency in *E. coli*. a** Efficiency of CRISPRt disruption of *sfgfp* in
1018 *E. coli* using a fluorescence phenotypic assay. The *E. coli yjaA-sfgfp-yjaB* strain (sJMP2688) is
1019 green fluorescent whereas the *E. coli* WT strain (sJMP163) is not. Isolates from CRISPRt
1020 targeted transposition of *E. coli yjaA-sfgfp-yjaB* with the *gfp1* guide (selection for
1021 transconjugants on LB-kan plates) were assayed for fluorescence; 82/84 (97.6%) were white
1022 indicating disruption of *sfgfp*. **b** Efficiency of CRISPRt disruption of *lacZ* in *E. coli* using an X-gal
1023 phenotypic assay. The *E. coli* WT strain (sJMP163) can metabolize X-gal resulting in a blue
1024 colony color whereas the *E. coli lacZYA* deletion strain (sJMP3272) cannot metabolize X-gal
1025 resulting in a white colony color. Isolates from CRISPRt targeted transposition of *E. coli* WT with
1026 the *LZ1* guide (selection for transconjugants on LB-kan plates) were assayed for colony color;
1027 90/90 (100%) were white indicating disruption of *lacZ*. **c** Efficiency of obtaining CRISPRt
1028 transconjugants in *E. coli* using the *LZ1* and *gfp1* guides. Serial dilutions of three technical
1029 replicates of *LZ1* and *gfp1* CRISPRt assays were plated with and without selection (LB-kan or
1030 LB, respectively) and CFUs were compared; Efficiency of CRISPRt targeted transposition in *E.*
1031 *coli* with the *LZ1* guide was ~1 in 100 and with the *gfp1* guide was ~1 in 1000.
1032
1033 **Fig. S3 Transcription impacts efficacy of CRISPRt guides. a.** No correlation between PAM
1034 sequence (CA, CC, CG, CT) and efficacy (frequency of insertion) for 46 *mScarlet-I* targeting
1035 guides. **b**. No correlation between CRISPRt guide position and efficacy for 46 *mScarlet-I*
1036 targeting guides. **c.** Schematic of *mScarlet-I* cassettes +/- promoter in *E. coli* chromosome. The

1037 *mScarlet-I* expression cassette (red) with and without a promoter (orange) along with a
1038 spectinomycin resistance cassette (SmR, brown) are located on the *E. coli* chromosome just
1039 downstream of *glmS* and upstream of *pstS*. The *mScarlet-I* expression cassette is inserted in
1040 one of two orientations so that the direction of transcription is either in the same or the opposite
1041 direction of the leading strand of chromosomal DNA replication. **d** Relative efficacy of CRISPRt
1042 *mScarlet-I* guides in a pooled screen targeting *mScarlet-I* expressed on the *E. coli* chromosome
1043 in different orientations with and without transcription. Relative efficacy is expressed as the log2-
1044 fold change of the frequency in the CRISPRt libraries (sJMP10519-10520, sJMP10594-10595,
1045 sJMP10637-10640) vs. the frequency in the original plasmid construct libraries (sJMP10505 and
1046 sJMP10506) shown on scatter plots.
1047
1048 **Fig. S4 Transcription impacts efficacy of CRISPRt guides. a** Relative efficacy of CRISPRt
1049 gRNAs in a pooled screen targeting *mScarlet-I* as in **Fig S3d** with average and standard
1050 deviation of two separate CRISPRt libraries (gentamicin^R and kanamycin^R) containing all 46
1051 guides shown. **b** Fluorescent phenotypes of 80 isolates from each of the *E. coli* CRISPRt
1052 *mScarlet-I* individual guide libraries (sJMP10641-10646) compared to *E. coli* strains with no
1053 *mScarlet-I* gene ((-) mScar, sJMP6999) or expressing *mScarlet-I* ((+) mScar, sJMP10205). Only
1054 4/480 (0.83%) retained *mScarlet-I* levels equal to the parent strain indicating an off-target rate of
1055 <1% overall.
1056
1057 **Fig. S5 CRISPRtOE construct details. a** Detailed schematic of the chromosomally-encoded
1058 promoterless *mScarlet-I* reporter contained on a Tn*7* transposon inserted into the att_{Tn7} site of *E.*
1059 *coli*. **b** Detailed schematics of CRISPRtOE Tn*7*-like transposon constructs with four different
1060 outward facing promoter sequences (no promoter, and constitutive promoters A, H, and V). **c**
1061 Sequence alignment of CRISPRtOE promoters A, H, and V compared to a consensus *E. coli* σ^{70}
1062 promoter. Promoter A is based on the *lacUV5* promoter. Promoter H and V are synthetic
1063 promoters. Promoter H has an UP element highlighted in yellow. **d** Schematic of CRISPRtOE
1064 transposon insertion into Landing Pad (LP) showing CRISPRtOE Promoter and transposon L-
1065 end relative to LP RBS and *mScarlet-I* coding sequence.
1066
1067 **Fig. S6 Tunable overexpression of chromosomally located genes using CRISPRtOE.**
1068 **a** mScarlet-I fluorescence analysis of *E. coli* CRISPRtOE isolates (no promoter or synthetic
1069 promoters A, V, and H) compared to the parent (promoterless *mScarlet-I*) strain. As in Fig 3b
1070 except values are shown for all CRISPRtOE isolates. **b** mScarlet-I fluorescence analysis of

1071 CRISPRtOE isolates of the Alphaproteobacterium *Zymomonas mobilis* (no promoter or synthetic
1072 promoters A, V, and H) compared to the parent (promoterless *mScarlet-I*) strain. Values are
1073 shown for isolates with on-target, RL orientation CRISPRtOE insertions. **c** Schematic showing
1074 insertion of CRISPRtOE transposon into the 'Landing Pad' upstream of *mScarlet-I*. Insertion
1075 position is variable (~45-55bp downstream of protospacer) resulting in a variable amount of the
1076 Landing Pad (containing the RBS) remaining upstream of the *mScarlet-I* coding sequence.
1077 Insertion positions and orientation of CRISPRtOE isolates in the eight species shown in Fig3 c.
1078 Insertion position is expressed relative to start of *mScarlet-I* coding sequence (equal to the
1079 remaining LP sequence).
1080
1081 **Fig. S7 CRISPRtOE *murA* pooled library screen and *folA* and *murA* MIC assays**. **a** Fitness
1082 of pooled strains overexpressing *murA* compared to the *lacZ* control strains in the presence of
1083 fosfomycin. **b** Schematic of CRISPRtOE insertion position upstream of genes. **c** MIC test strip
1084 assays (trimethoprim, 0.002-32 µg/ml) comparing WT and CRISPRtOE *folA* isolates. **d** MIC test
1085 strip assays (fosfomycin, 0.064-1024 µg/ml) comparing WT and CRISPRtOE *murA* isolates.
1086
1087 **Fig. S8 CRISPRtOE reproducibility. a** Biological replicates of CRISPRtOE data at the gene
1088 level. **b** Replicate comparison of TMP treatment versus DMSO control. FC = fold change. **c**
1089 Comparison of TMP versus DMSO for the promoter H versus no promoter libraries.
1090
1091 **Fig. S9 CRISPRtOE robustness with fewer analyzed guides.** Scatterplots comparing all
1092 spacers measured in our study to subsets of 5, 4, 3, or 2 randomly selected spacers per gene.
1093
1094 **Fig. S10 CRISPRtOE TMP screen positive and negative outlier genes. a** Top positive gene
1095 hits in TMP treatment only considering the first gene in the operon. Genes must have at least a
1096 4-fold change in the promoter H data and show a 4-fold difference in a comparison between
1097 promoter H and no promoter to be considered. **b** Genes from the enriched STRING group "DNA
1098 binding HTH domain, AraC-type, and Transcription regulators MarR/SlyA-like" (CL:3238) as well
1099 as *acrA*. **c** Genes from the enriched GO group "Enterobacterial common antigen biosynthetic
1100 process" (GO:0009246) as well as *metF* and *folM*. Error bars represent standard deviation (SD).

Fig 1

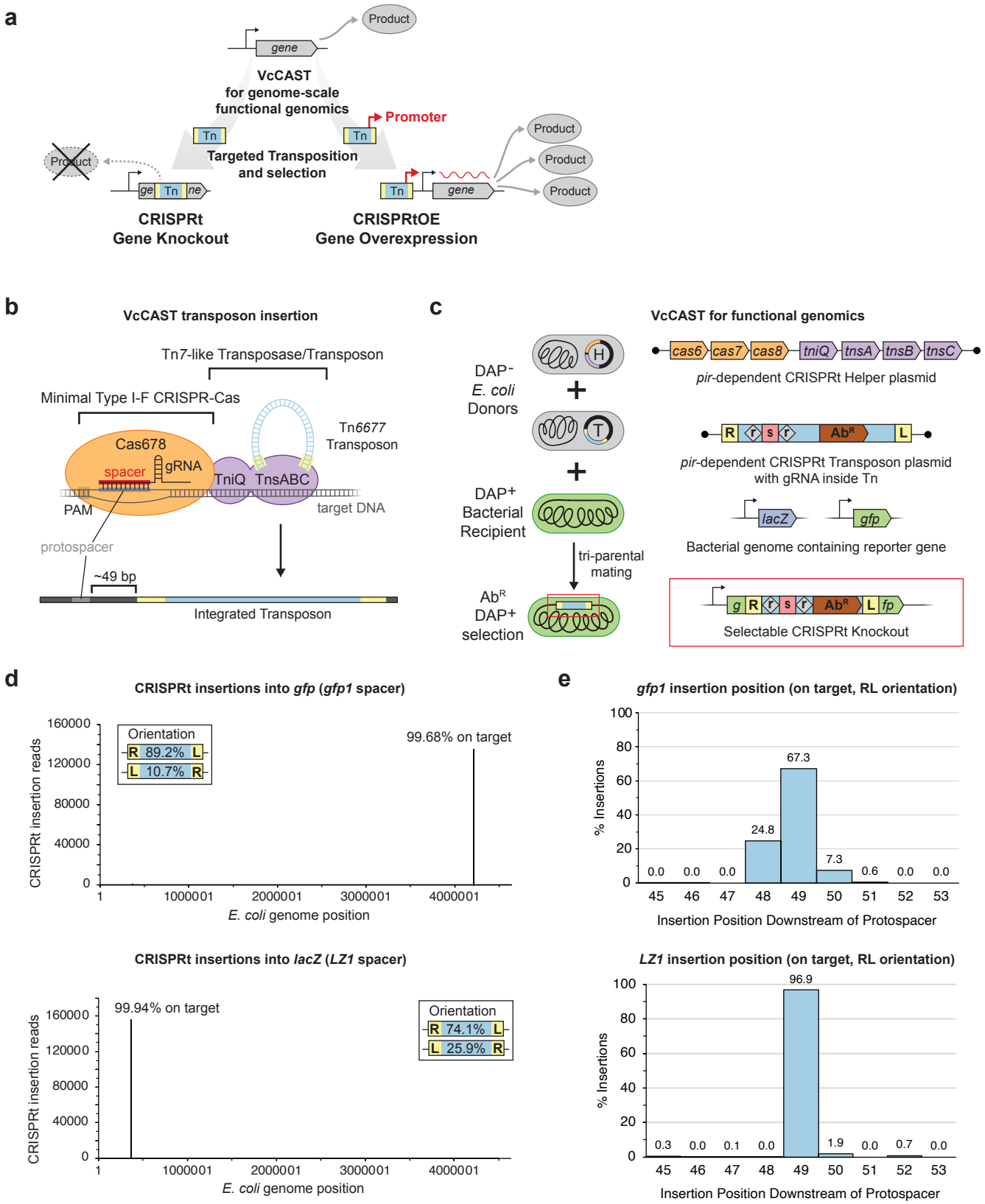
a
Product
gene
VcCAST
for genome-scale
functional genomics
Promoter
Tn
Tn
Product
Product
Product
Product
Targeted Transposition
and selection
ge
Tn
ne
Tn
gene
CRISPRt
Gene Knockout
CRISPRtOE
Gene Overexpression
b
VcCAST transposon insertion
Tn7-like Transposase/Transposon
Minimal Type I-F CRISPR-Cas
Tn6677
Transposon
Cas678
gRNA
spacer
TniQ
TnsABC
PAM
target DNA
protospacer
~49 bp
Integrated Transposon
c
VcCAST for functional genomics
DAP⁻
E. coli
Donors
H
T
DAP⁺
Bacterial
Recipient
tri-parental
mating
AbR
DAP⁺
selection
cas6
cas7
cas8
tniQ
tnsA
tnsB
tnsC
pir-dependent CRISPRt Helper plasmid
R
r
s
r
AbR
L
pir-dependent CRISPRt Transposon plasmid
with gRNA inside Tn
lacZ
gfp
Bacterial genome containing reporter gene
g
R
r
s
r
AbR
L
fp
Selectable CRISPRt Knockout
d
CRISPRt insertions into gfp (gfp1 spacer)
CRISPRt insertion reads
160000
120000
80000
40000
0
Orientation
R 89.2% L
L 10.7% R
99.68% on target
1
1000001
2000001
3000001
4000001
E. coli genome position
CRISPRt insertions into lacZ (LZ1 spacer)
CRISPRt insertion reads
160000
120000
80000
40000
0
99.94% on target
Orientation
R 74.1% L
L 25.9% R
1
1000001
2000001
3000001
4000001
E. coli genome position
e
gfp1 insertion position (on target, RL orientation)
% Insertions
100
80
60
40
20
0
0.0
0.0
0.0
24.8
67.3
7.3
0.6
0.0
0.0
45
46
47
48
49
50
51
52
53
Insertion Position Downstream of Protospacer
LZ1 insertion position (on target, RL orientation)
% Insertions
100
80
60
40
20
0
0.3
0.0
0.1
0.0
96.9
1.9
0.0
0.7
0.0
45
46
47
48
49
50
51
52
53
Insertion Position Downstream of Protospacer

Fig 2

a

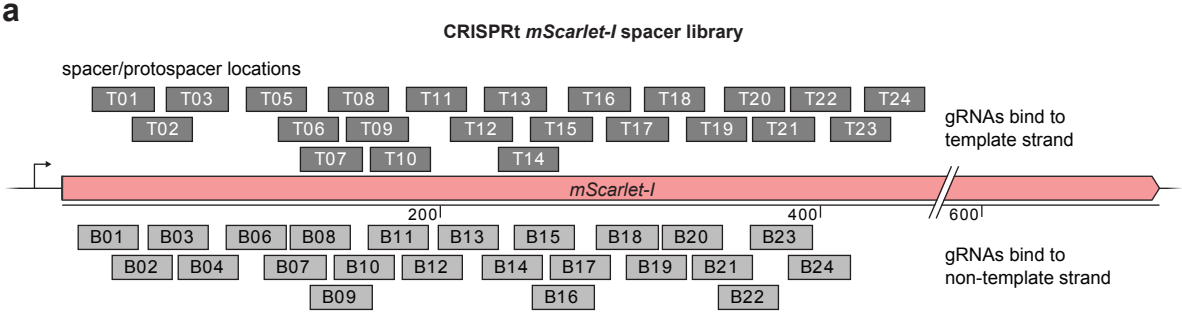
CRISPRt mScarlet-I spacer library
spacer/protospacer locations
T01 T03 T05 T08 T11 T13 T16 T18 T20 T22 T24
T02 T06 T09 T12 T15 T17 T19 T21 T23
T07 T10 T14
gRNAs bind to template strand
mScarlet-I
200
400
600
B01 B03 B06 B08 B11 B13 B15 B18 B20 B23
B02 B04 B07 B10 B12 B14 B17 B19 B21 B24
B09 B16 B22
gRNAs bind to non-template strand

b

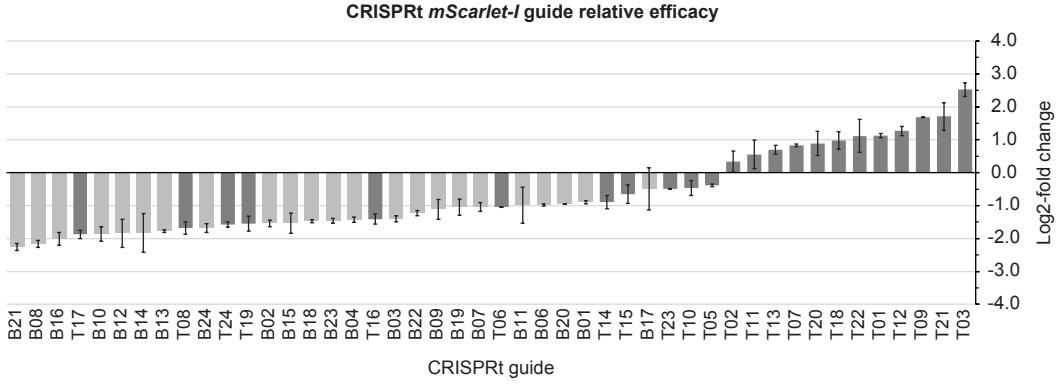
CRISPRt mScarlet-I guide relative efficacy
4.0
3.0
2.0
1.0
0.0
-1.0
-2.0
-3.0
-4.0
Log2-fold change
B21 B08 B16 T17 B10 B12 B14 B13 T08 B24 T24 T19 B02 B15 B18 B23 B04 T16 B03 B22 B09 B19 B07 T06 B11 B06 B20 B01 T14 T15 B17 T23 T10 T05 T02 T11 T13 T07 T20 T18 T22 T01 T12 T09 T21 T03
CRISPRt guide

c

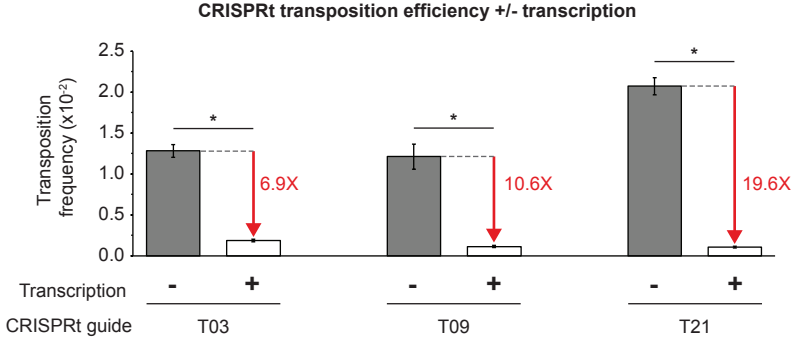
CRISPRt transposition efficiency +/- transcription
Transposition frequency (x10-2)
2.5
2.0
1.5
1.0
0.5
0.0
*
6.9X
10.6X
19.6X
Transcription
-
+
CRISPRt guide
T03
T09
T21

Fig 3

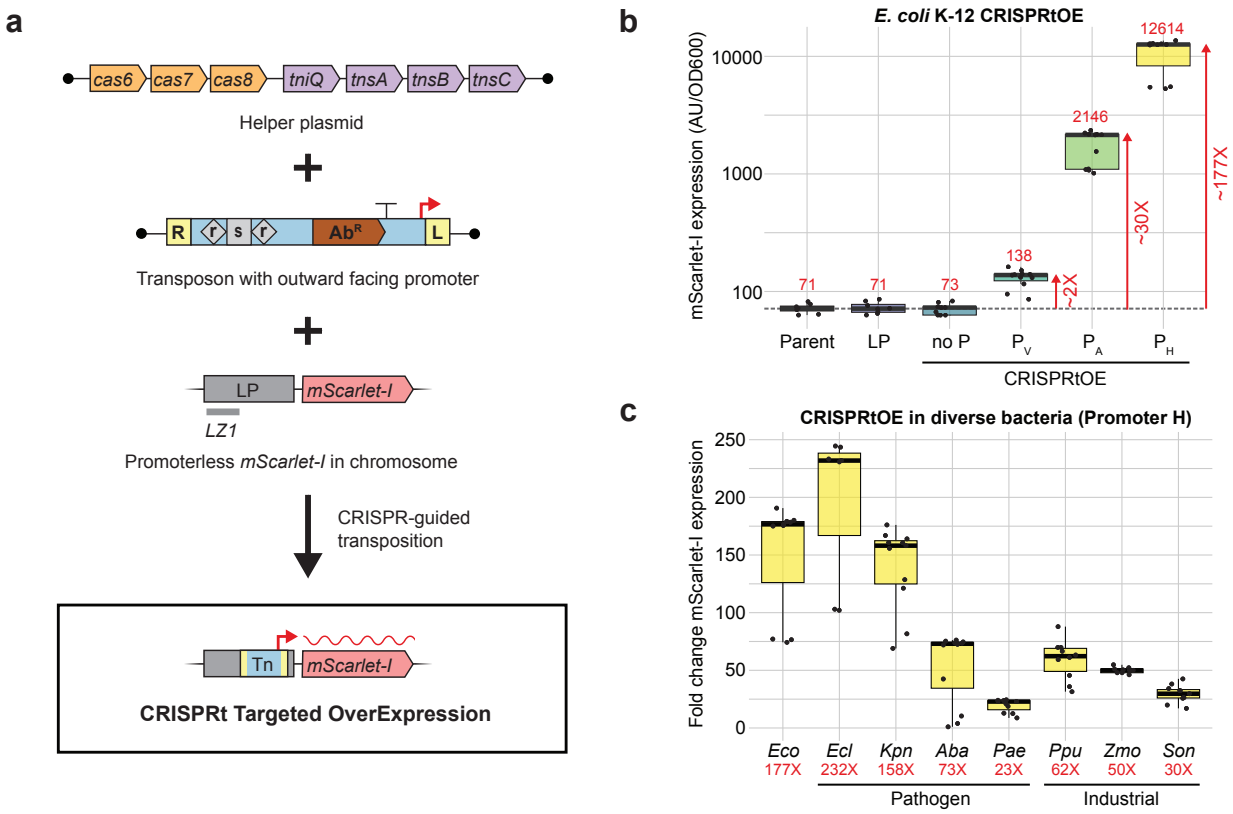
a
cas6
cas7
cas8
tniQ
tnsA
tnsB
tnsC
Helper plasmid
R
r
s
r
Ab^R
L
Transposon with outward facing promoter
LP
mScarlet-I
LZ1
Promoterless mScarlet-I in chromosome
CRISPR-guided transposition
Tn
mScarlet-I
CRISPRt Targeted OverExpression
b
E. coli K-12 CRISPRtOE
mScarlet-I expression (AU/OD600)
10000
1000
100
71
71
73
138
2146
12614
~2X
~30X
~177X
Parent
LP
no P
P_V
P_A
P_H
CRISPRtOE
c
CRISPRtOE in diverse bacteria (Promoter H)
Fold change mScarlet-I expression
250
200
150
100
50
0
Eco 177X
Ecl 232X
Kpn 158X
Aba 73X
Pae 23X
Ppu 62X
Zmo 50X
Son 30X
Pathogen
Industrial

Fig 4

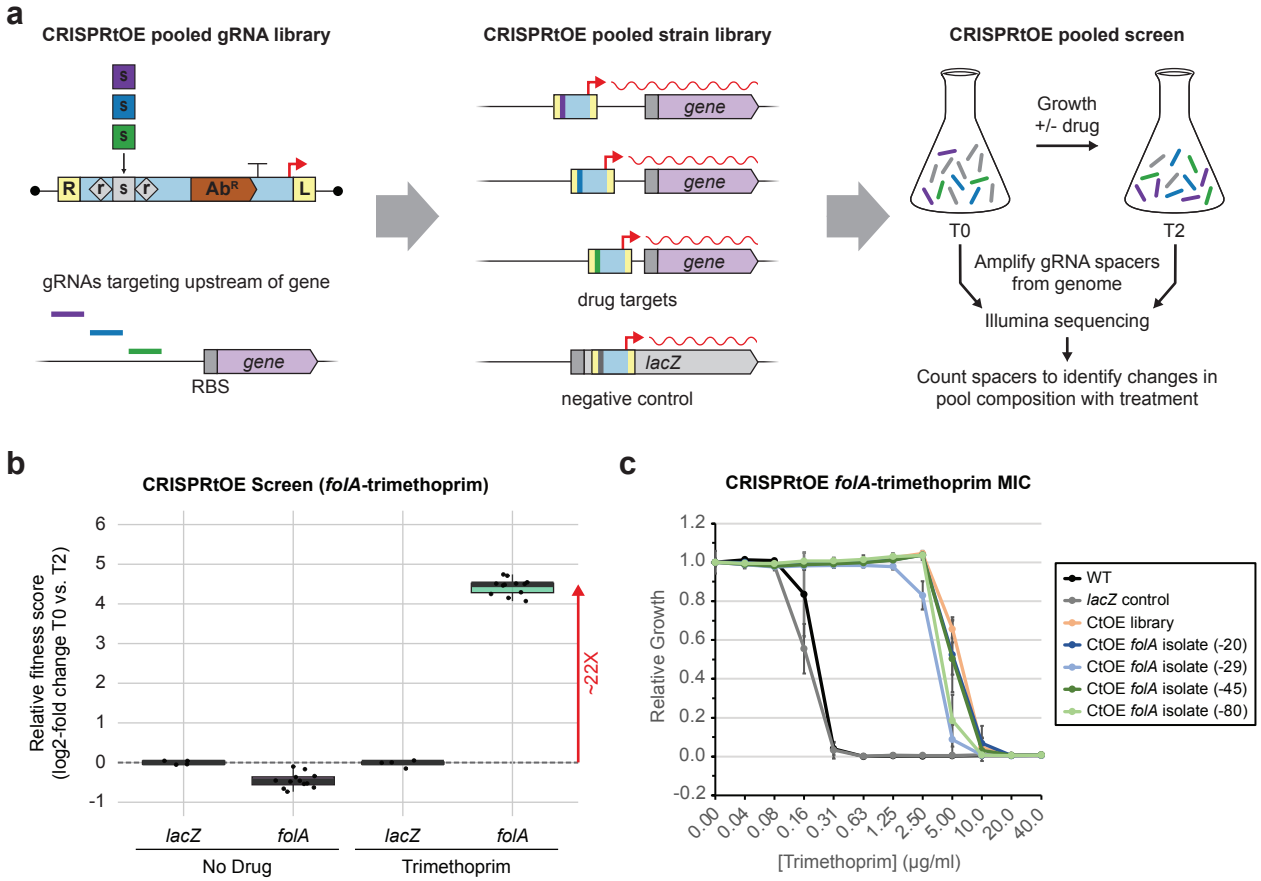
a
CRISPRtOE pooled gRNA library
s
s
s
R
r
s
r
Ab^R
L
gRNAs targeting upstream of gene
gene
RBS
CRISPRtOE pooled strain library
gene
gene
gene
drug targets
lacZ
negative control
CRISPRtOE pooled screen
Growth
+/- drug
T0
T2
Amplify gRNA spacers
from genome
Illumina sequencing
Count spacers to identify changes in
pool composition with treatment
b
CRISPRtOE Screen (folA-trimethoprim)
Relative fitness score
(log2-fold change T0 vs. T2)
6
5
4
3
2
1
0
-1
~22X
lacZ
folA
lacZ
folA
No Drug
Trimethoprim
c
CRISPRtOE folA-trimethoprim MIC
Relative Growth
1.2
1.0
0.8
0.6
0.4
0.2
0.0
-0.2
0.00
0.04
0.08
0.16
0.31
0.63
1.25
2.50
5.00
10.0
20.0
40.0
[Trimethoprim] (µg/ml)
WT
lacZ control
CtOE library
CtOE folA isolate (-20)
CtOE folA isolate (-29)
CtOE folA isolate (-45)
CtOE folA isolate (-80)

Fig 5

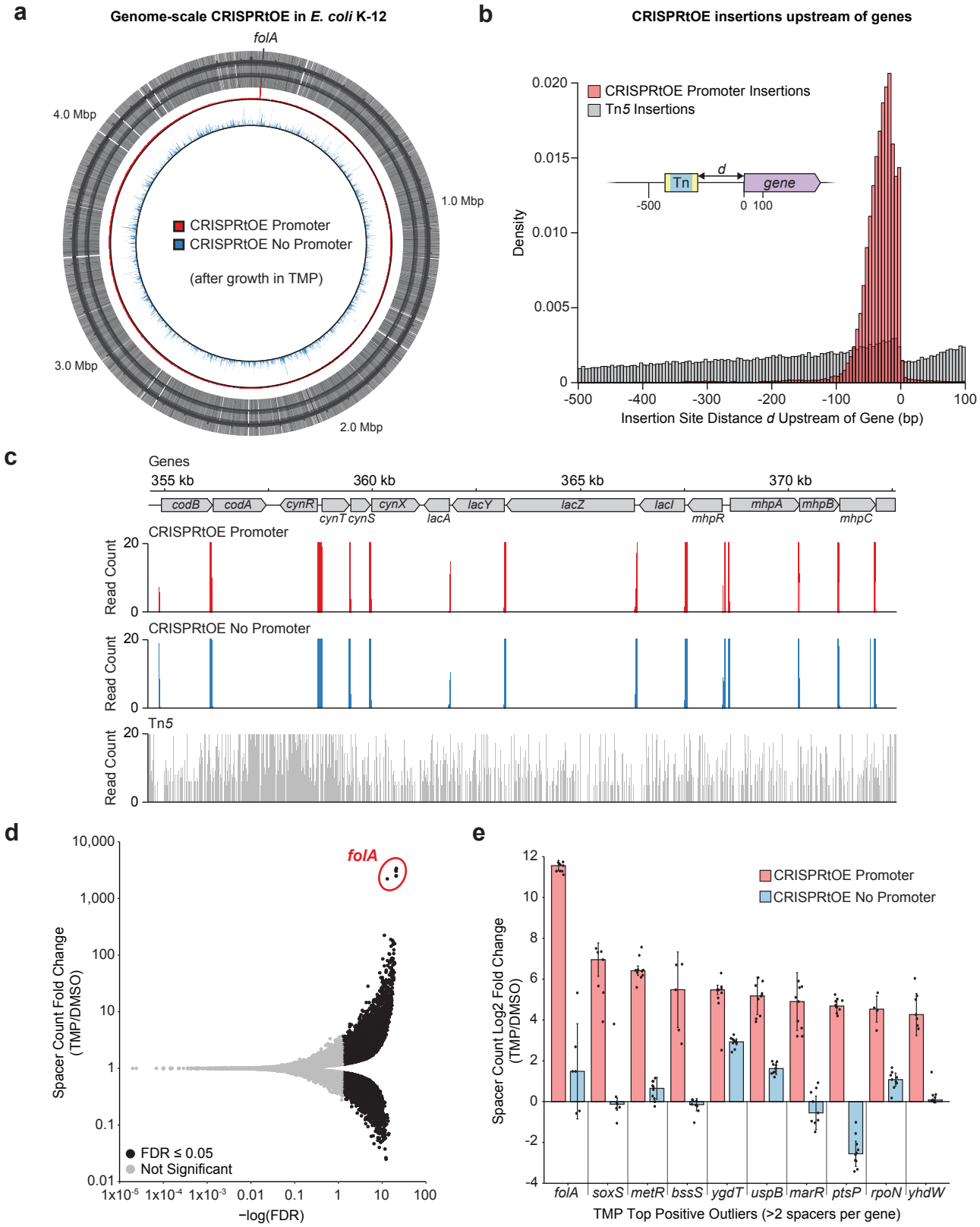
a
Genome-scale CRISPRtOE in E. coli K-12
folA
4.0 Mbp
1.0 Mbp
3.0 Mbp
2.0 Mbp
CRISPRtOE Promoter
CRISPRtOE No Promoter
(after growth in TMP)
b
CRISPRtOE insertions upstream of genes
CRISPRtOE Promoter Insertions
Tn5 Insertions
Tn
d
gene
-500
0 100
Density
Insertion Site Distance d Upstream of Gene (bp)
c
Genes
355 kb
360 kb
365 kb
370 kb
codB
codA
cynR
cynT cynS
cynX
lacA
lacY
lacZ
lacI
mhpR
mhpA
mhpB
mhpC
CRISPRtOE Promoter
CRISPRtOE No Promoter
Tn5
Read Count
d
folA
Spacer Count Fold Change (TMP/DMSO)
FDR ≤ 0.05
Not Significant
−log(FDR)
e
CRISPRtOE Promoter
CRISPRtOE No Promoter
Spacer Count Log2 Fold Change (TMP/DMSO)
folA
soxS
metR
bssS
ygdT
uspB
marR
ptsP
rpoN
yhdW
TMP Top Positive Outliers (>2 spacers per gene)

Fig S1

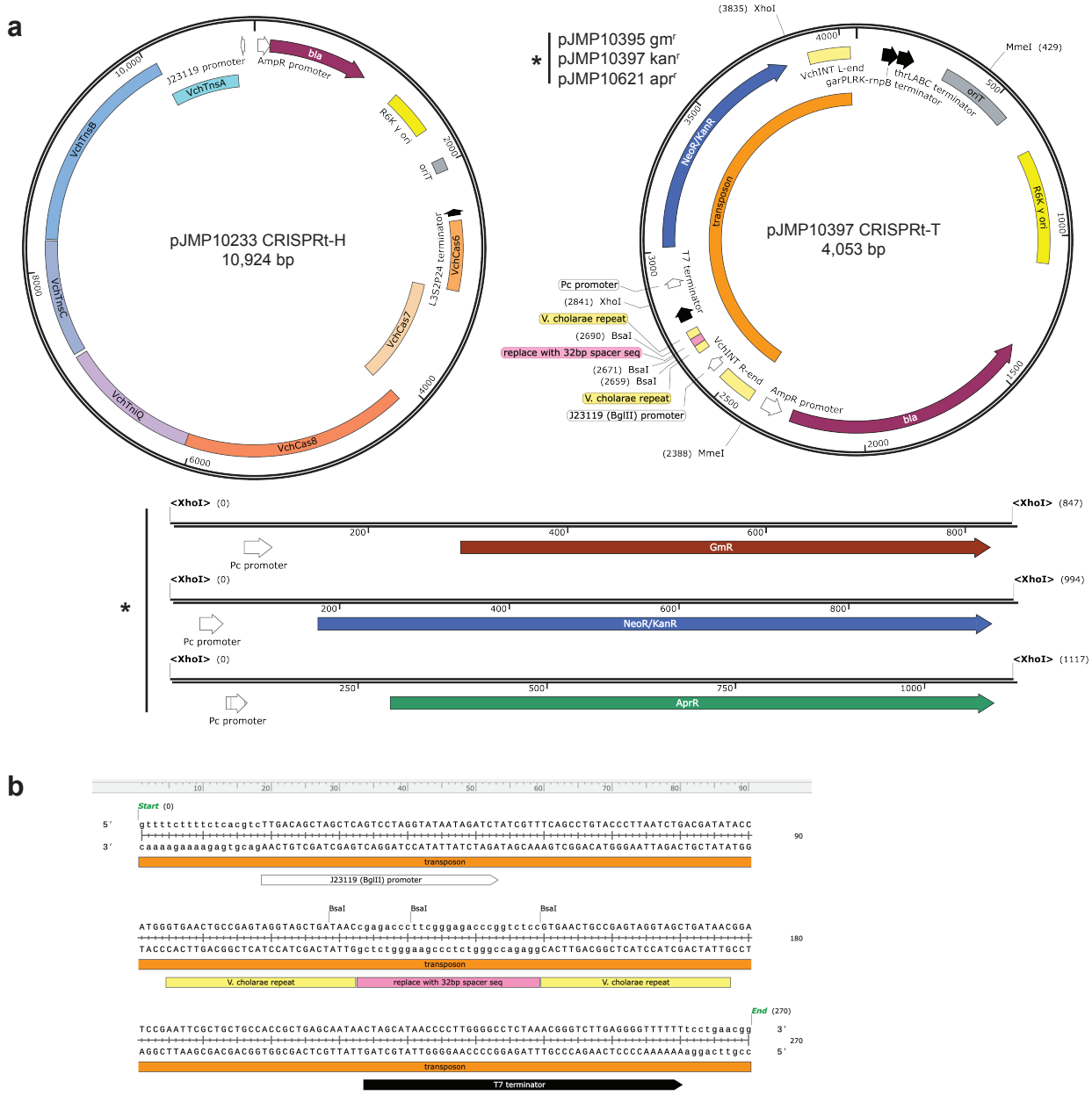
a
pJMP10233 CRISPRt-H
10,924 bp
J23119 promoter
AmpR promoter
bla
VchTnsA
VchTnsB
VchTnsC
VchTnsD
R6K γ ori
oriT
L3S2P24 terminator
VchCas6
VchCas7
VchCas8
10,000
8000
6000
4000
2000
*
pJMP10395 gmr
pJMP10397 kanr
pJMP10621 apr
pJMP10397 CRISPRt-T
4,053 bp
(3835) XhoI
MmeI (429)
VchINT L-end
garPLRK-rnpB terminator
thrLABC terminator
oriT
R6K γ ori
NeoR/KanR
transposon
T7 terminator
Pc promoter
(2841) XhoI
V. cholarae repeat
(2690) BsaI
replace with 32bp spacer seq
(2671) BsaI
(2659) BsaI
V. cholarae repeat
J23119 (BglII) promoter
VchINT R-end
AmpR promoter
bla
(2388) MmeI
4000
3500
3000
2500
2000
1500
1000
<XhoI> (0)
<XhoI> (847)
GmR
Pc promoter
<XhoI> (0)
<XhoI> (994)
NeoR/KanR
Pc promoter
<XhoI> (0)
<XhoI> (1117)
AprR
Pc promoter
b
Start (0)
5′ gttttcttttctcacgtcTTGACAGCTAGCTCAGTCCTAGGTATAATAGATCTATCGTTTCAGCCTGTACCCTTAATCTGACGATATACC
3′ caaaagaaaagagtgcagAACTGTCGATCGAGTCAGGATCCATATTATCTAGATAGCAAAGTCGGACATGGGAATTAGACTGCTATATGG
transposon
J23119 (BglII) promoter
BsaI
BsaI
BsaI
ATGGGTGAACTGCCGAGTAGGTAGCTGATAACcgagacccttcgggagacccggtctccGTGAACTGCCGAGTAGGTAGCTGATAACGGA
TACCCACTTGACGGCTCATCCATCGACTATTGgctctgggaagccctctgggccagaggCACTTGACGGCTCATCCATCGACTATTGCCT
transposon
V. cholarae repeat
replace with 32bp spacer seq
V. cholarae repeat
End (270)
TCCGAATTCGCTGCTGCCACCGCTGAGCAATAACTAGCATAACCCCTTGGGGCCTCTAAACGGGTCTTGAGGGGTTTTTTtcctgaacgg 3′
AGGCTTAAGCGACGACGGTGGCGACTCGTTATTGATCGTATTGGGGAACCCCGGAGATTTGCCCAGAACTCCCCAAAAAAaggacttgcc 5′
transposon
T7 terminator
c
250
500
750
1000
1250
yjaA
GFP expression cassette insertion
yjaB
superfolder GFP
thrLABC terminator
Pveg promoter
L3S1P13 terminator
FRT scar (cmR cassette removed)
L3S2P24 terminator

Fig S2

a

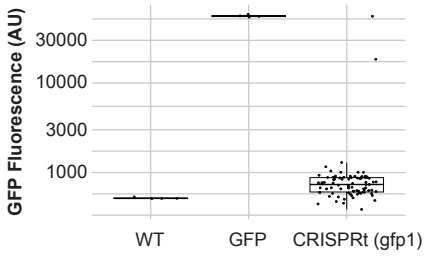

Strain	Parent Strain genotype	CRISPRt guide	Fluorescence phenotype
sJMP163	E. coli MG1655 WT	na	white
sJMP2688	E. coli MG1655 gfp	na	green
isolates	E. coli MG1655 gfp	gfp1	82/84 white (97.6% gfp disruption)

b

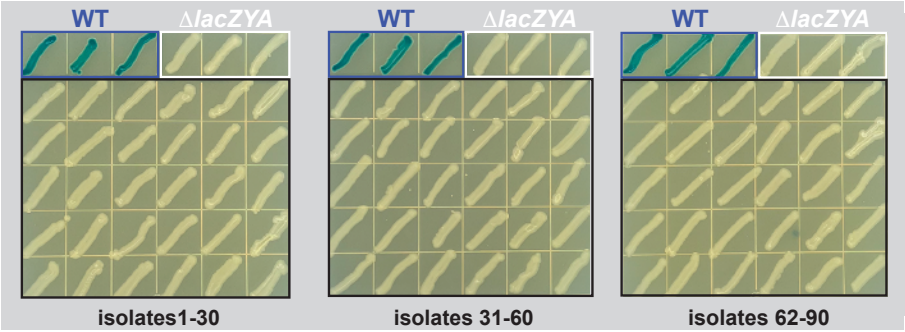

Strain	Parent Strain genotype	CRISPRt guide	X-gal phenotype
sJMP163	E. coli MG1655 WT	na	blue
sJMP3272	E. coli MG1655 DlacZYA	na	white
isolates	E. coli MG1655 WT	LZ1	90/90 white (100% lacZ disruption)

c

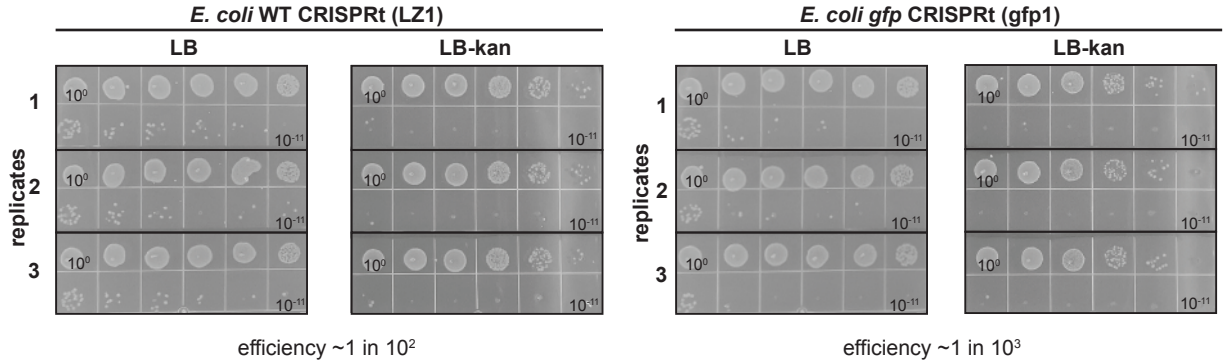

Fig S3

a

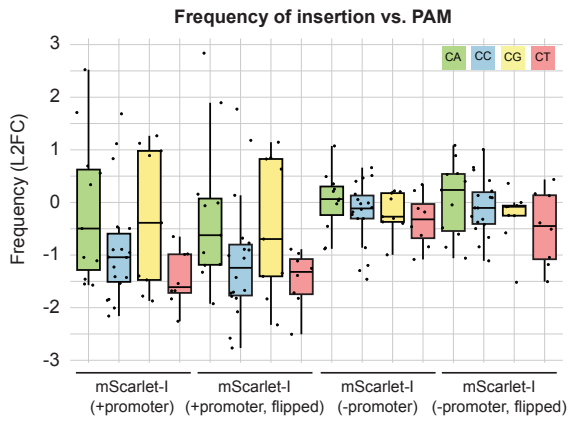

b

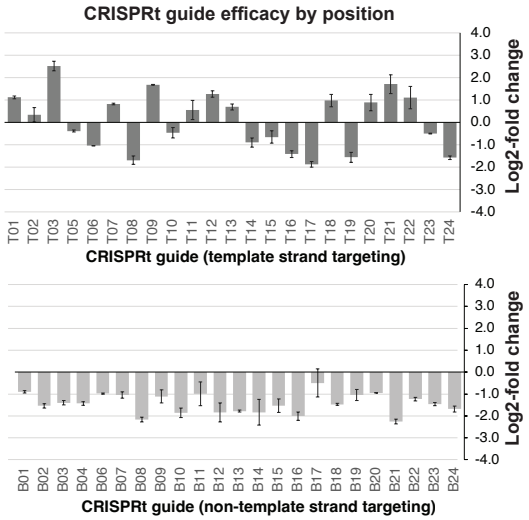

c

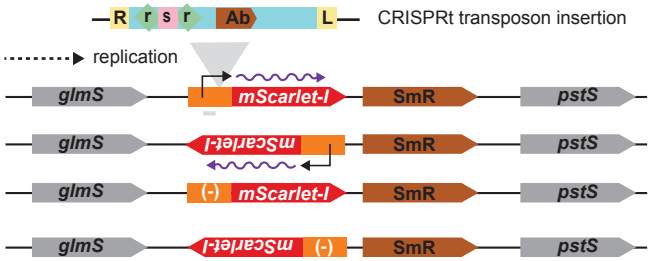

DNA strand	Promoter
leading	+
lagging	+
leading	-
lagging	-

d

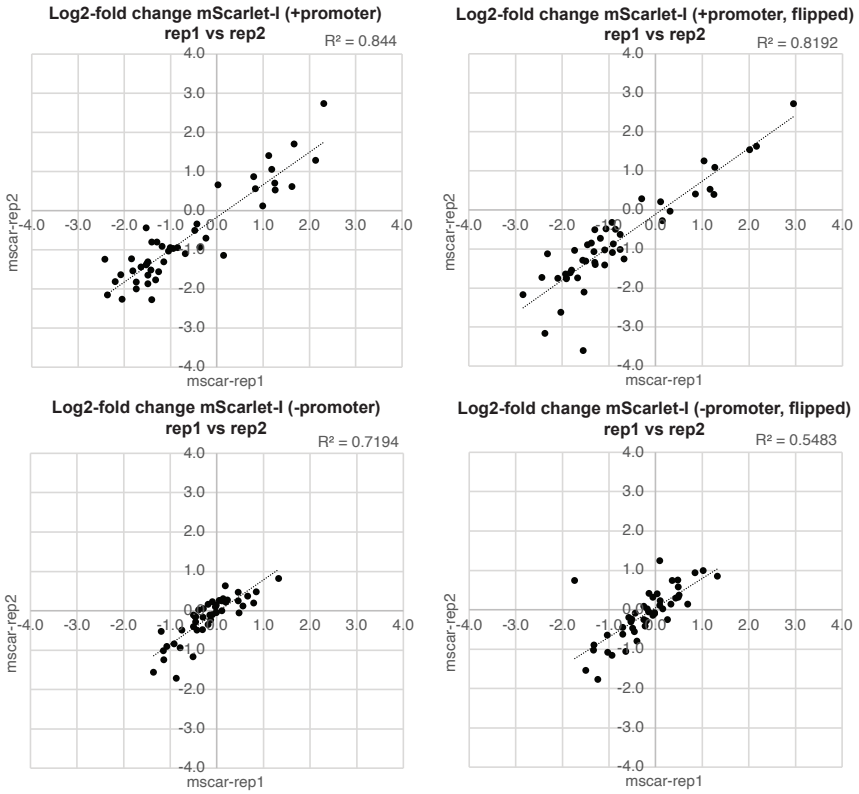

Fig S4

a

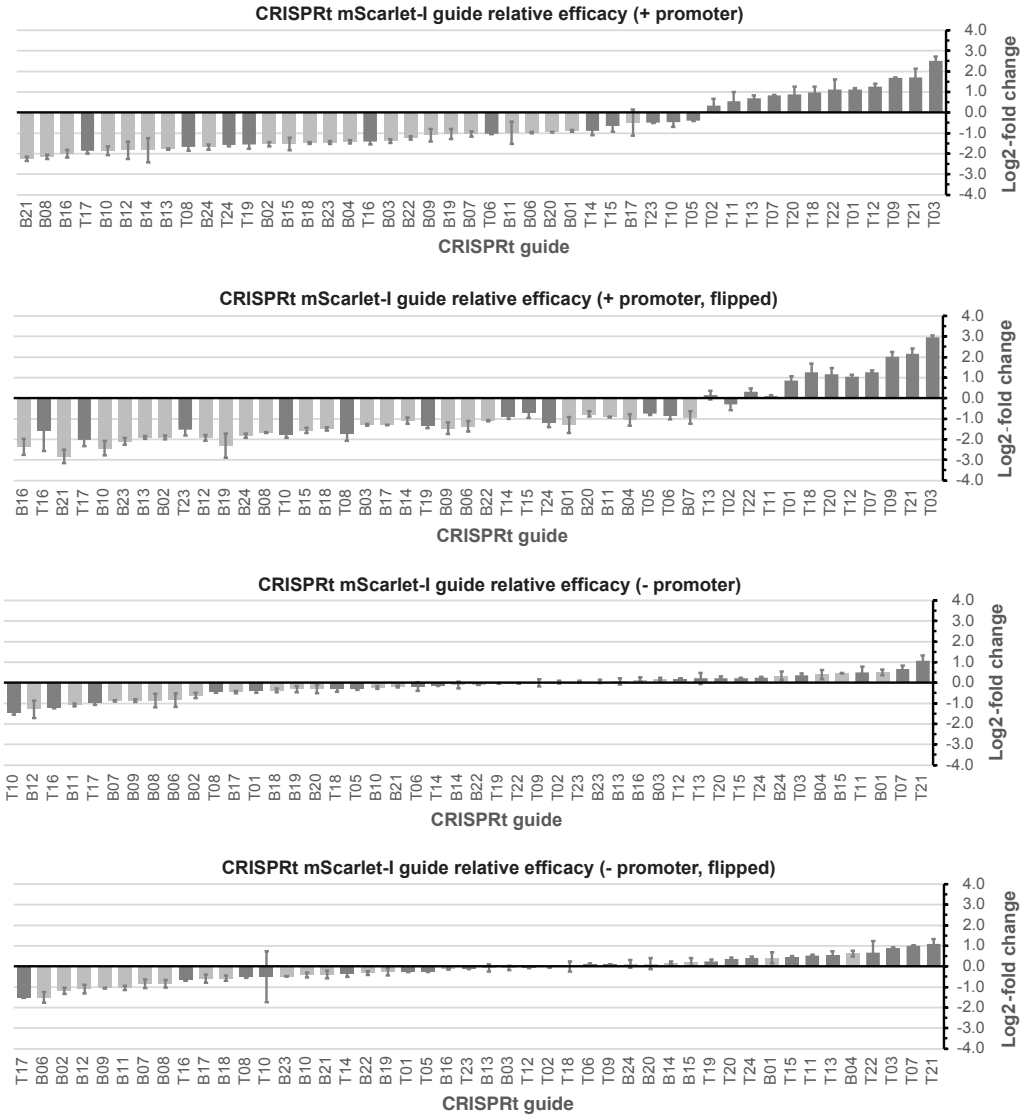
CRISPRt mScarlet-I guide relative efficacy (+ promoter)
Log2-fold change
4.0
3.0
2.0
1.0
0.0
-1.0
-2.0
-3.0
-4.0
B21 B08 B16 T17 B10 B12 B14 B13 T08 B24 T24 T19 B02 B15 B18 B23 B04 T16 B03 B22 B09 B19 B07 T06 B11 B06 B20 B01 T14 T15 B17 T23 T10 T05 T02 T11 T13 T07 T20 T18 T22 T01 T12 T09 T21 T03
CRISPRt guide
CRISPRt mScarlet-I guide relative efficacy (+ promoter, flipped)
Log2-fold change
B16 T16 B21 T17 B10 B23 B13 B02 T23 B12 B19 B24 B08 T10 B15 B18 T08 B03 B17 B14 T19 B09 B06 B22 T14 T15 T24 B01 B20 B11 B04 T05 T06 B07 T13 T02 T22 T11 T01 T18 T20 T12 T07 T09 T21 T03
CRISPRt guide
CRISPRt mScarlet-I guide relative efficacy (- promoter)
Log2-fold change
T10 B12 T16 B11 T17 B07 B09 B08 B06 B02 T08 B17 T01 B18 B19 B20 T18 T05 B10 B21 T06 T14 B14 B22 T19 T22 T09 T02 T23 B23 B13 B16 B03 T12 T13 T20 T15 T24 B24 T03 B04 B15 T11 B01 T07 T21
CRISPRt guide
CRISPRt mScarlet-I guide relative efficacy (- promoter, flipped)
Log2-fold change
T17 B06 B02 B12 B09 B11 B07 B08 T16 B17 B18 T08 T10 B23 B10 B21 T14 B22 B19 T01 T05 B16 T23 B13 B03 T12 T02 T18 T06 T09 B24 B20 B14 B15 T19 T20 T24 B01 T15 T11 T13 B04 T22 T03 T07 T21
CRISPRt guide

b

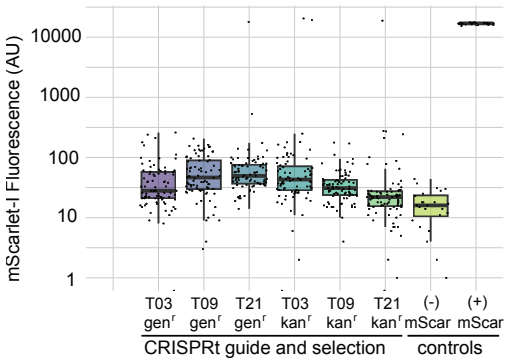
mScarlet-I Fluorescence (AU)
10000
1000
100
10
1
T03 gen^r
T09 gen^r
T21 gen^r
T03 kan^r
T09 kan^r
T21 kan^r
(-) mScar
(+) mScar
CRISPRt guide and selection
controls

Fig S5

a

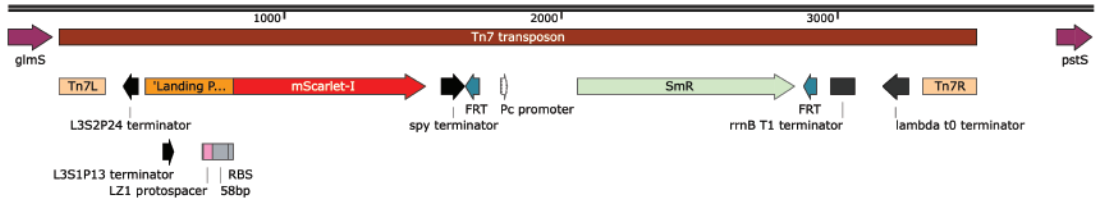

b

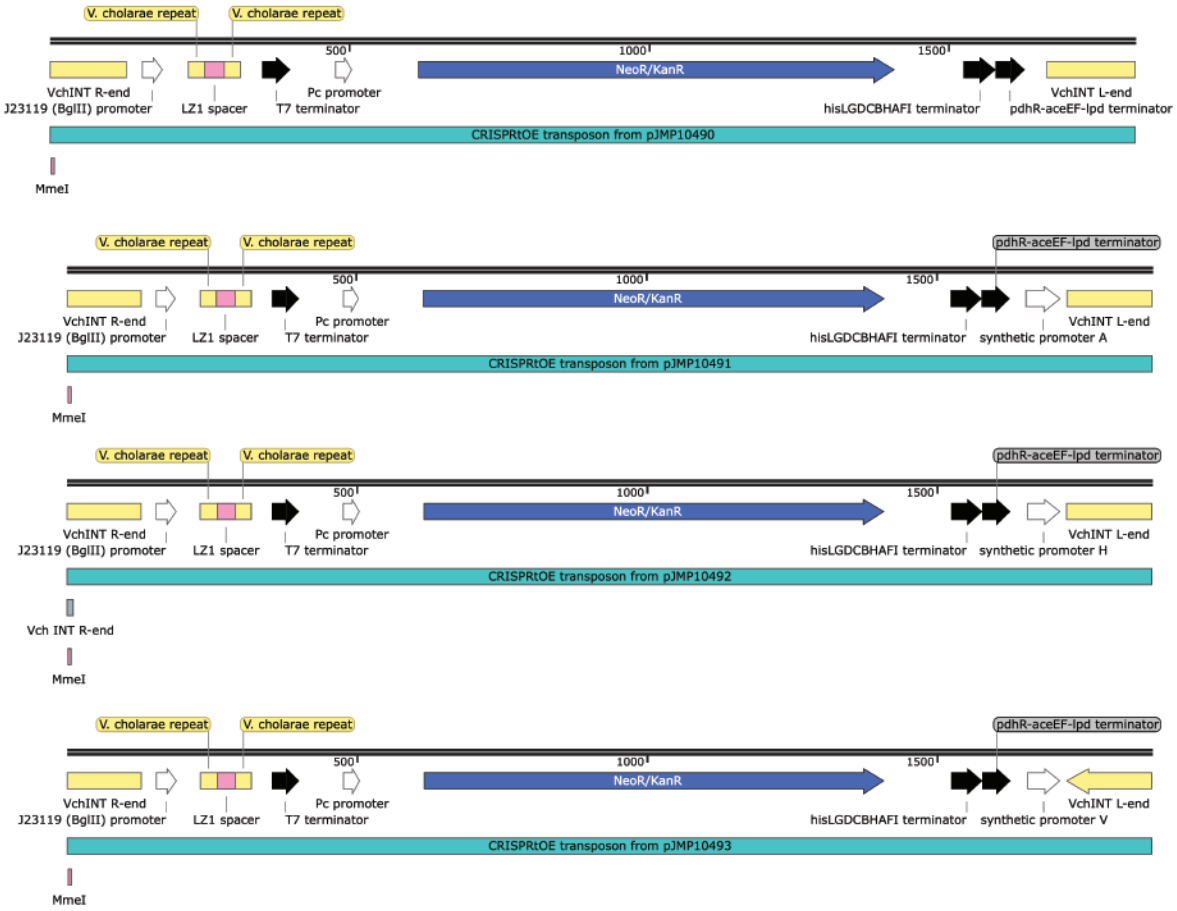

c

CRISPRtOE Promoter Sequences

```
A  CTCACTCATTAGGCACCCCAGGCTTTACACTTTATGCTTCCGGCTCGTATAATGTCTAG
H  GGAAAATTTTTTTTCAAAAGTACTTGAAAATTAATCA•TCCGGCTCGTATAATTCTAGT
V  CACCAAGCCAGTTACCTCGGTTCTTTAATCTTTATGC•TCCGGCTCGTATAGTGCTAGC
   nnnnnnnnnnnnnnnnnnnnnnnTTGACAnnnnnnnn•nnnnnnnnnTATAATnnnnnn
                              -35        spacer        -10
```

Fig S6

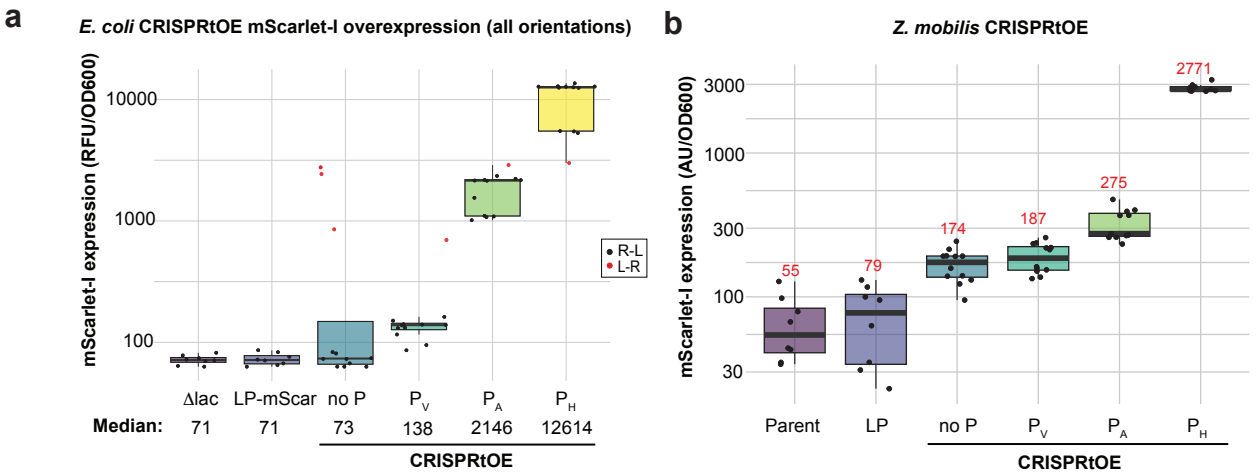

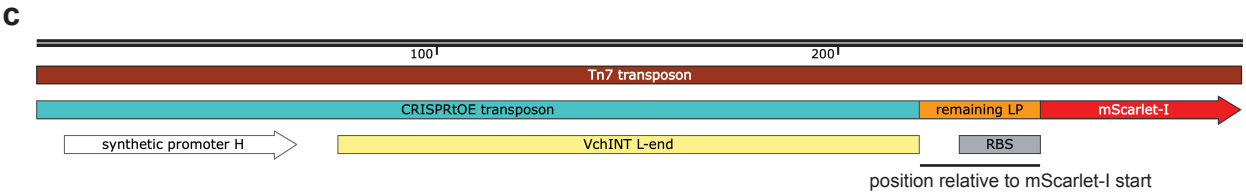

Position of CRISPRtOE transposon in Landing Pad relative to mScarlet-I start (LZ1 guide)

	# insertions analyzed	RL vs LR orientation		Position relative to ATG start (% of total RL insertions)									
	total RL and LR	%RL	%LR	-35	-34	-33	-32	-31	-30	-13	-2	+19	+108
Eco	48	87.5	12.5	21.4	2.4	71.4	0.0	0.0	4.8	0.0	0.0	0.0	0.0
Aba	12	100.0	0.0	0.0	0.0	66.7	0.0	0.0	0.0	8.3	8.3	8.3	8.3
Ecl	8	87.5	12.5	28.6	0.0	71.4	0.0	0.0	0.0	0.0	0.0	0.0	0.0
Kpn	10	90.0	10.0	22.2	0.0	77.8	0.0	0.0	0.0	0.0	0.0	0.0	0.0
Pae	12	91.7	8.3	36.4	0.0	63.6	0.0	0.0	0.0	0.0	0.0	0.0	0.0
Ppu	12	83.3	16.7	10.0	10.0	80.0	0.0	0.0	0.0	0.0	0.0	0.0	0.0
Son	11	100.0	0.0	36.4	9.1	45.5	0.0	0.0	9.1	0.0	0.0	0.0	0.0
Zmo	48	91.7	8.3	0.0	2.3	95.5	2.3	0.0	0.0	0.0	0.0	0.0	0.0

Fig S7

a

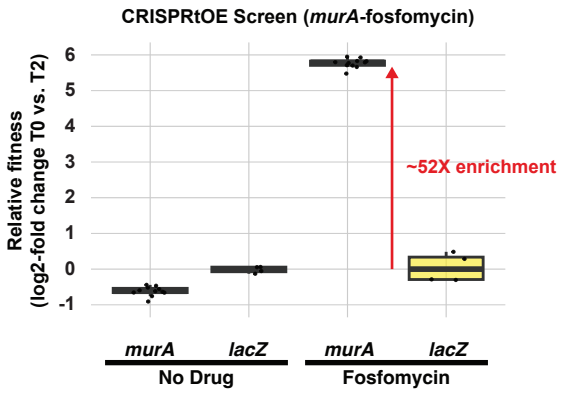

b

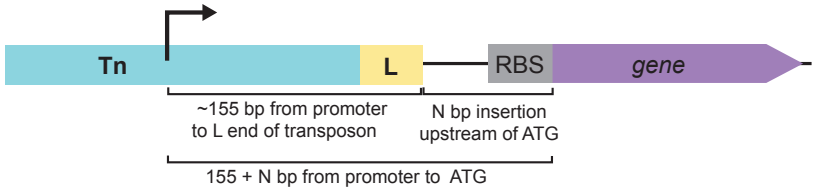

c Trimethoprim MIC (0.002-32 µg/ml)

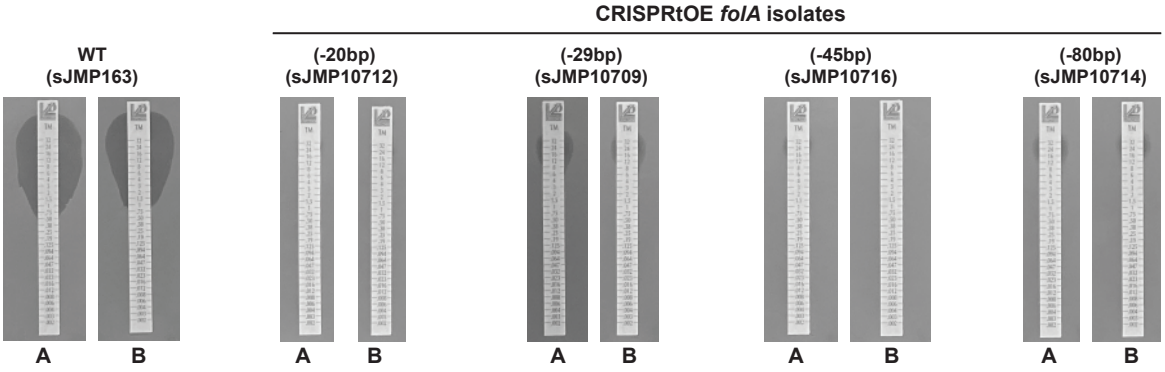

d Fosfomycin MIC (0.064-1024 µg/ml)

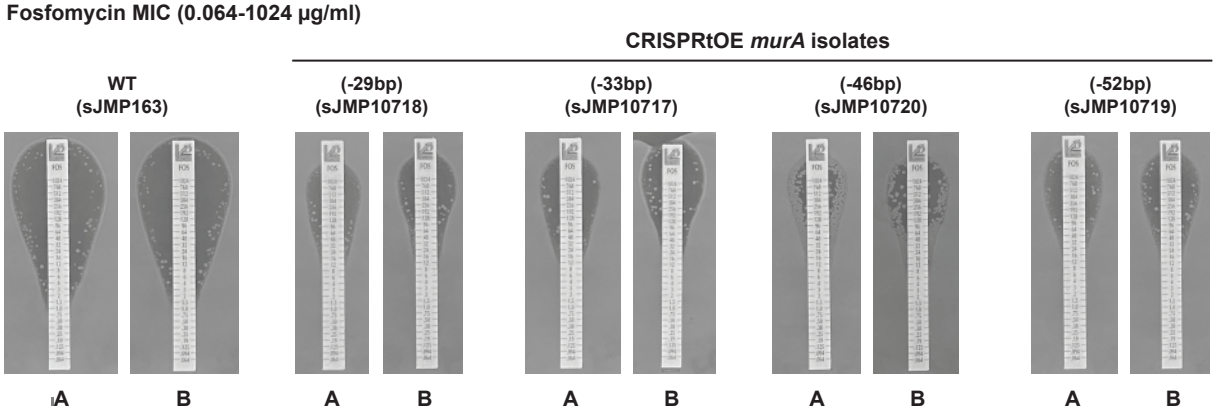

Fig S8

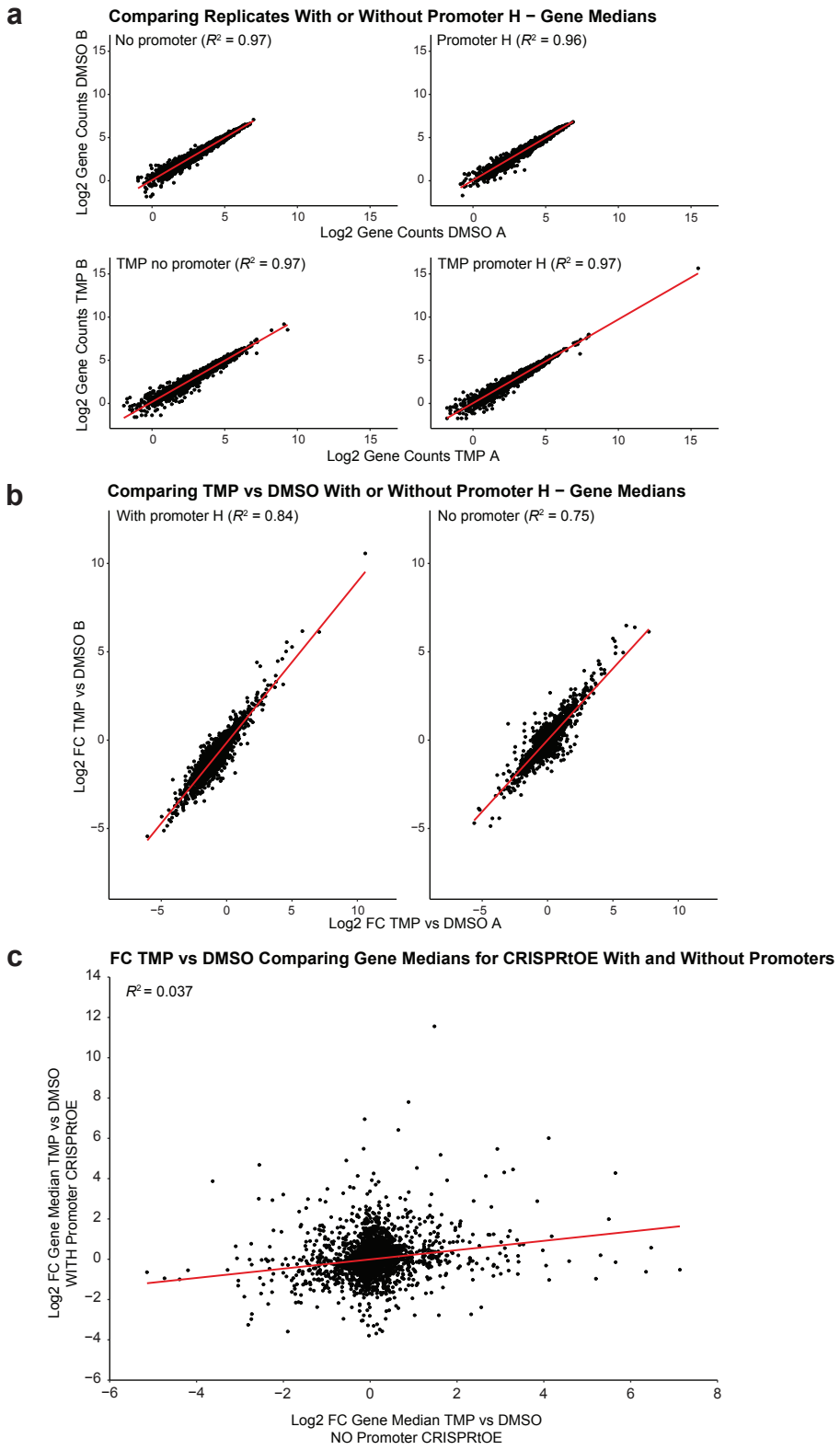
a
Comparing Replicates With or Without Promoter H − Gene Medians
No promoter (R^2 = 0.97)
Promoter H (R^2 = 0.96)
TMP no promoter (R^2 = 0.97)
TMP promoter H (R^2 = 0.97)
Log2 Gene Counts DMSO B
Log2 Gene Counts DMSO A
Log2 Gene Counts TMP B
Log2 Gene Counts TMP A
b
Comparing TMP vs DMSO With or Without Promoter H − Gene Medians
With promoter H (R^2 = 0.84)
No promoter (R^2 = 0.75)
Log2 FC TMP vs DMSO B
Log2 FC TMP vs DMSO A
c
FC TMP vs DMSO Comparing Gene Medians for CRISPRtOE With and Without Promoters
R^2 = 0.037
Log2 FC Gene Median TMP vs DMSO WITH Promoter CRISPRtOE
Log2 FC Gene Median TMP vs DMSO NO Promoter CRISPRtOE

Fig S9

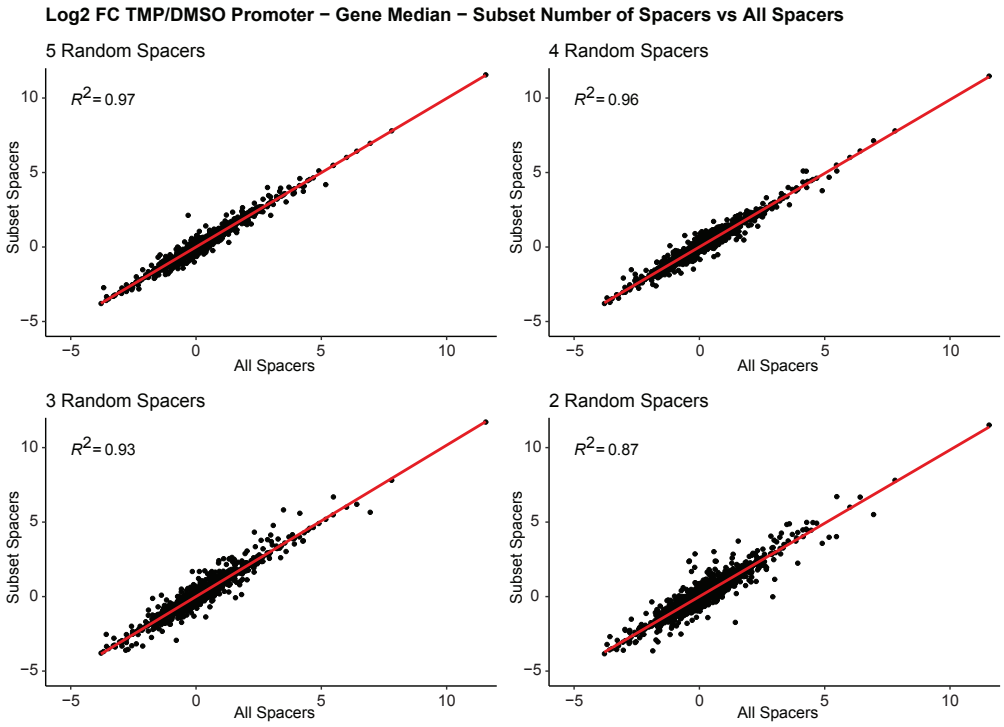
Log2 FC TMP/DMSO Promoter − Gene Median − Subset Number of Spacers vs All Spacers
5 Random Spacers
R^2= 0.97
4 Random Spacers
R^2= 0.96
3 Random Spacers
R^2= 0.93
2 Random Spacers
R^2= 0.87
Subset Spacers
All Spacers
−5
0
5
10

Fig S10

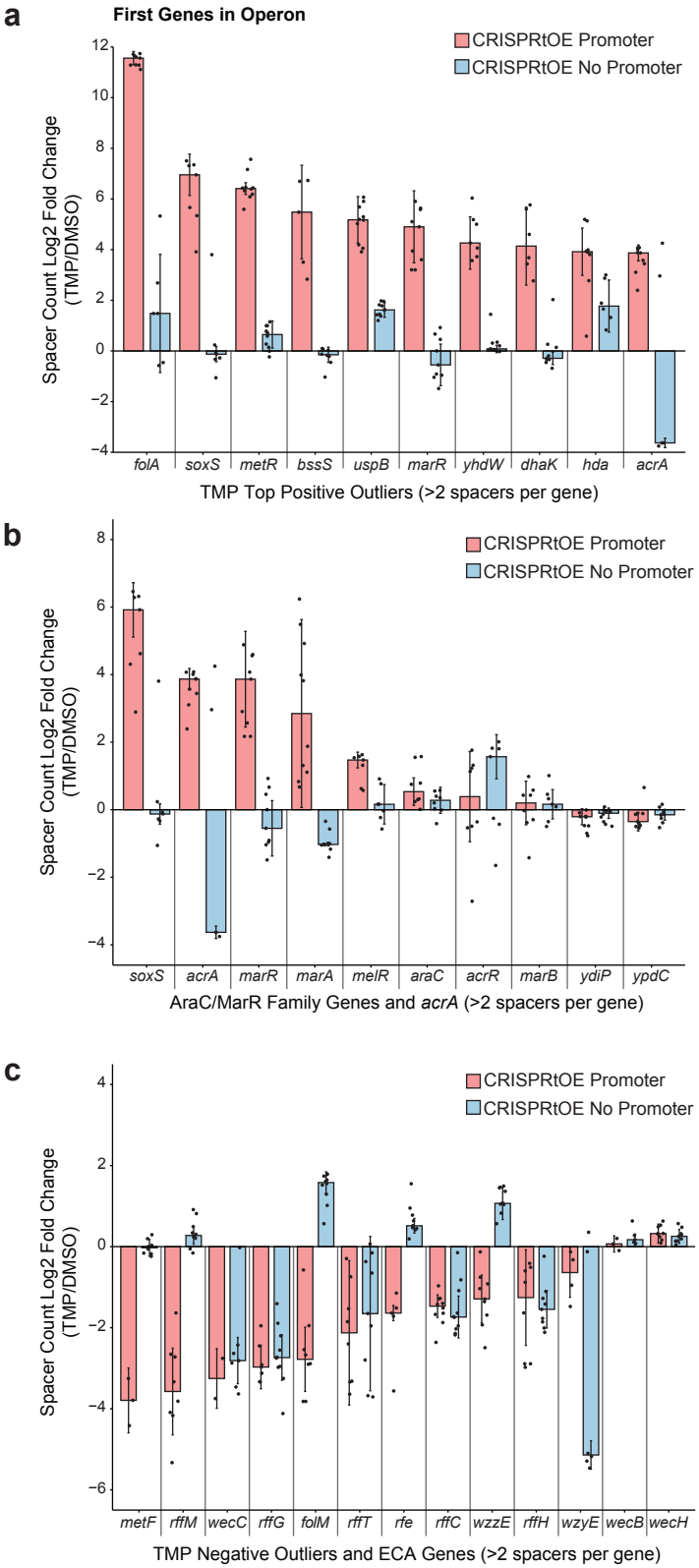
a
First Genes in Operon
CRISPRtOE Promoter
CRISPRtOE No Promoter
Spacer Count Log2 Fold Change (TMP/DMSO)
folA
soxS
metR
bssS
uspB
marR
yhdW
dhaK
hda
acrA
TMP Top Positive Outliers (>2 spacers per gene)
b
CRISPRtOE Promoter
CRISPRtOE No Promoter
Spacer Count Log2 Fold Change (TMP/DMSO)
soxS
acrA
marR
marA
melR
araC
acrR
marB
ydiP
ypdC
AraC/MarR Family Genes and acrA (>2 spacers per gene)
c
CRISPRtOE Promoter
CRISPRtOE No Promoter
Spacer Count Log2 Fold Change (TMP/DMSO)
metF
rffM
wecC
rffG
folM
rffT
rfe
rffC
wzzE
rffH
wzyE
wecB
wecH
TMP Negative Outliers and ECA Genes (>2 spacers per gene)